MID-AMERICA TRANSPORTATION CENTER

Report # MATC-UNL: 004-22

Final Report

WBS: 21-1121-0005-004-22

Virtual Barriers for Mitigating and Preventing Run-Off-Road Crashes - Phase II

Cody Stolle, PhD
Midwest Roadside Safety Facility
Research Assistant Professor
Department of Mechanical and Materials Engineering
University of Nebraska-Lincoln

Ronald K. Faller, PhD, PE
MwRSF Director
Research Professor
Department of Civil & Environmental Engineering

Michael Sweigard, BSME
Graduate Student, MwRSF
Department of Mechanical Engineering

Ricardo Jacome, BSME
Graduate Student, MwRSF
Department of Mechanical Engineering

2020

A Cooperative Research Project sponsored by U.S. Department of Transportation- Office of the Assistant Secretary for Research and Technology

MATC

Virtual Barriers for Mitigating and Preventing Run-Off-Road Crashes Phase II

Cody Stolle, Ph.D.
Midwest Roadside Safety Facility (MwRSF)
Research Assistant Professor
Department of Mechanical and Materials Engineering
University of Nebraska-Lincoln

Ronald K. Faller, Ph.D., P.E.
MwRSF Director
Research Professor
Department of Civil & Environmental Engineering
University of Nebraska-Lincoln

Michael Sweigard, B.S.M.E.
Graduate Student, MwRSF
Department of Mechanical Engineering
University of Nebraska-Lincoln

Ricardo Jacome, B.S.M.E.
Graduate Student, MwRSF
Department of Mechanical Engineering
University of Nebraska-Lincoln

A Report on Research Sponsored by

Mid-America Transportation Center
University of Nebraska–Lincoln

February 2020

TECHNICAL REPORT DOCUMENTATION PAGE

1. Report No. 21-1121-0005-004-22	2.	3. Recipient's Accession No.
4. Title and Subtitle Virtual Barriers for Mitigating and Preventing Run-Off-Road Crashes Phase II		5. Report Date February 2020
		6.
7. Author(s) Cody Stolle, PhD ORCID: 0000-0001-6674-7383 Ronald Faller, PhD, P.E. ORCID: 0000-0001-7660-1572 Michael Sweigard, B.S.M.E. Ricardo Jacome, B.S.M.E.		8. Performing Organization Report No. 21-1121-0005-004-22
9. Performing Organization Name and Address Midwest Roadside Safety Facility (MwRSF) Nebraska Transportation Center University of Nebraska-Lincoln Main Office: Prem S. Paul Research Center at Whittier School Room 130, 2200 Vine Street Lincoln, Nebraska 68583-0853 Outdoor Test Site: 4630 NW 36th Street Lincoln, Nebraska 68524		10. Project/Task/Work Unit No. 11. Contract (C) or Grant (G) No. 69A3551747107
12. Sponsoring Organization Name and Address Office of the Assistant Secretary for Research and Technology 1200 New Jersey Ave., SE Washington, D.C. 20590		13. Type of Report and Period Covered Final Report: 2018-2019 14. Sponsoring Agency Code MATC TRB RiP No. 91994-30
15. Supplementary Notes Prepared in cooperation with U.S. Department of Transportation, Federal Highway Administration.		

16. Abstract

This research study describes progress made during a multi-year evaluation of concepts to prevent vehicles from departing the roadway. During Phase 2, researchers identified potential methods of interpreting road coordinates using vehicle dynamics concepts. Current intelligent technology was investigated to learn about the current status of technology and evaluate potential system gaps and flaws to develop a supplementary system.

The second phase of this project proposes a novel method to offer an extra level of redundancy to current vehicle guidance systems. The method is separated into three main modules denoted as: Local Path Generation, Local Positioning, and Vehicle Guidance/Warning. The Local Path Generation module explored techniques to wirelessly convey road data to a vehicle while requiring the minimum amount of data and transmission time. The guidance information is collected to develop a local road database and referenced locally, geospatially, and relative to other adjacent road segments. As well, the vehicle instantaneous position is identified using the Local Positioning module, in which the coordinates of the vehicle can be quickly related in terms of position, speed, and orientation with respect to the roadway with minimal lag. The Vehicle Guidance System module is the reaction system which compares data from Local Path Generation and Local Positioning modules to determine if the risk of roadside departure exceeds an unacceptable level of risk, and responds by notifying the driver and/or performing safety maneuvers to control the vehicle path. Feasibility and application of these modules and concepts were explored and further research recommendations were provided for the third and final year of MATC funding.

17. Document Analysis/Descriptors Highway Safety, Run off road crashes, Path Prediction, Vehicle Controls, Inter-Vehicle Communication, Traffic Management		18. Availability Statement No restrictions. Document available from: National Technical Information Services, Springfield, Virginia 22161	
19. Security Class (this report) Unclassified	20. Security Class (this page) Unclassified	21. No. of Pages 99	22. Price

SI* (MODERN METRIC) CONVERSION FACTORS

APPROXIMATE CONVERSIONS TO SI UNITS

Symbol	When You Know	Multiply By	To Find	Symbol
		LENGTH		
in.	inches	25.4	millimeters	mm
ft	feet	0.305	meters	m
yd	yards	0.914	meters	m
mi	miles	1.61	kilometers	km
		AREA		
in^2	square inches	645.2	square millimeters	mm^2
ft^2	square feet	0.093	square meters	m^2
yd^2	square yard	0.836	square meters	m^2
ac	acres	0.405	hectares	ha
mi^2	square miles	2.59	square kilometers	km^2
		VOLUME		
fl oz	fluid ounces	29.57	milliliters	mL
gal	gallons	3.785	liters	L
ft^3	cubic feet	0.028	cubic meters	m^3
yd^3	cubic yards	0.765	cubic meters	m^3
		1 NOTE: volumes greater than 1,000 L shall be shown in m^3		
		MASS		
oz	ounces	28.35	grams	g
lb	pounds	0.454	kilograms	kg
T	short ton (2,000 lb)	0.907	megagrams (or “metric ton”)	Mg (or "t")
		TEMPERATURE (exact degrees)		
°F	Fahrenheit	5(F-32)/9 or (F-32)/1.8	Celsius	°C
		ILLUMINATION		
fc	foot-candles	10.76	lux	lx
fl	foot-Lamberts	3.426	candela per square meter	cd/m^2
		FORCE & PRESSURE or STRESS		
lbf	poundforce	4.45	newtons	N
lbf/in^2	poundforce per square inch	6.89	kilopascals	kPa

APPROXIMATE CONVERSIONS FROM SI UNITS

Symbol	When You Know	Multiply By	To Find	Symbol
		LENGTH		
mm	millimeters	0.039	inches	in.
m	meters	3.28	feet	ft
m	meters	1.09	yards	yd
km	kilometers	0.621	miles	mi
		AREA		
mm^2	square millimeters	0.0016	square inches	in^2
m^2	square meters	10.764	square feet	ft^2
m^2	square meters	1.195	square yard	yd^2
ha	hectares	2.47	acres	ac
km^2	square kilometers	0.386	square miles	mi^2
		VOLUME		
mL	milliliter	0.034	fluid ounces	fl oz
L	liters	0.264	gallons	gal
m^3	cubic meters	35.314	cubic feet	ft^3
m^3	cubic meters	1.307	cubic yards	yd^3
		MASS		
g	grams	0.035	ounces	oz
kg	kilograms	2.202	pounds	lb
Mg (or "t")	megagrams (or “metric ton”)	1.103	short ton (2,000 lb)	T
		TEMPERATURE (exact degrees)		
°C	Celsius	1.8C+32	Fahrenheit	°F
		ILLUMINATION		
lx	lux	0.0929	foot-candles	fc
cd/m^2	candela per square meter	0.2919	foot-Lamberts	fl
		FORCE & PRESSURE or STRESS		
N	newtons	0.225	poundforce	lbf
kPa	kilopascals	0.145	poundforce per square inch	lbf/in^2

*SI is the symbol for the International System of Units. Appropriate rounding should be made to comply with Section 4 of ASTM E380.

Table of contents

List of Figures

List of Tables

Abstract

This research study describes progress made during a multi-year evaluation of concepts to prevent vehicles from departing the roadway. During Phase 2, researchers identified potential methods of interpreting road coordinates using vehicle dynamics concepts. Current intelligent technology was investigated to learn about the current status of technology and evaluate potential system gaps and flaws to develop a supplementary system.

The second phase of this project proposes a novel method to offer an extra level of redundancy to current vehicle guidance systems. The method is separated into three main modules denoted as: Local Path Generation, Local Positioning, and Vehicle Guidance/Warning. The Local Path Generation module explored techniques to wirelessly convey road data to a vehicle while requiring the minimum amount of data and transmission time. The guidance information is collected to develop a local road database and referenced locally, geospatially, and relative to other adjacent road segments. As well, the vehicle instantaneous position is identified using the Local Positioning module, in which the coordinates of the vehicle can be quickly related in terms of position, speed, and orientation with respect to the roadway with minimal lag. The Vehicle Guidance System module is the reaction system which compares data from Local Path Generation and Local Positioning modules to determine if the risk of roadside departure exceeds an unacceptable level of risk, and responds by notifying the driver and/or performing safety maneuvers to control the vehicle path. Feasibility and application of these modules and concepts were explored and further research recommendations were provided for the third and final year of MATC funding.

Disclaimer Statement

This report was completed with funding from the Mid-American Transportation Center. The contents of this report reflect the views and opinions of the authors who are responsible for the facts and the accuracy of the data presented herein. The contents do not necessarily reflect the official views or policies of the Mid-American Transportation Center. This report does not constitute a standard, specification, regulation, product endorsement, or an endorsement of manufacturers.

Acknowledgements

The authors wish to acknowledge several sources that made a contribution to this project: (1) Mid-America Transportation Center.; (2) Richard Stepp at Florida DOT; (3) David Boruff at Indiana DOT; (4) Erik Emerson at Wisconsin DOT; and (5) Phil Tenhulzen at Nebraska DOT.

Acknowledgement is also given to the following individuals who contributed to the completion of this research project.

Midwest Roadside Safety Facility

J.D. Reid, Ph.D., Professor
J.D. Schmidt, Ph.D., P.E., Research Assistant Professor
J.C. Holloway, M.S.C.E., E.I.T., Test Site Manager
K.A. Lechtenberg, M.S.M.E., E.I.T., Research Engineer
R.W. Bielenberg, M.S.M.E., E.I.T., Research Engineer
S.K. Rosenbaugh, M.S.C.E., E.I.T., Research Engineer
A.T. Russell, B.S.B.A., Testing and Maintenance Technician II
S.M. Tighe, Construction and Testing Technician I
D.S. Charroin, Construction and Testing Technician I
M.A. Rasmussen, Former Construction and Testing Technician I
E.W. Krier, Construction and Testing Technician II
M.T. Ramel, Construction and Testing Technician I
R.M. Novak, Construction and Testing Technician I
J.E. Kohtz, B.S.M.E., CAD Technician
E.L. Urbank, B.A., Research Communication Specialist
Undergraduate and Graduate Research Assistants

Chapter 1 Introduction

1.1 Problem Statement

The Federal Highway Administration (FHWA) reported that approximately 53% of fatal crashes (18,779) between 2014 and 2016 were related to roadside departures or lane departures [1]. According to the National Highway Traffic Safety Administration (NHTSA) *Fatal Accident Reporting System* (FARS) statistics [2] and the Insurance Institute for Highway Safety (IIHS) and Highway Loss Data Institute (HLDI) annual compilations [3], approximately 10,000 fatal run-off-road (ROR) crashes occur each year involving roadside fixed objects. As a result, ROR fixed-object fatal crashes account for approximately 1/3 of all fatal crashes. Cross-median crashes are among the most deadly type of ROR crash, in which a vehicle exits the travelway and crosses a median, striking an opposing vehicle from the opposite travel direction.

Non-fatal ROR crashes are also concerning and economically devastating. Research conducted at the University of Nebraska-Lincoln identified approximately 440,000 crashes involving only roadside trees and utility poles in a five-year period spanning twelve geographically dissimilar states [4]. It was determined that the United States experiences an estimated $13 to 17 billion in direct (emergency medical services, first responders, cleanup, infrastructure repairs) and indirect costs (traffic congestion, loss of work days and taxable income, incapacitation, lawsuits) related only to non-fatal roadside tree and utility pole crashes every year.

Researchers with experience in roadside crash reconstruction reviewed ROR crash data, including vehicle trajectories, during the Year 1 study of the Virtual Barriers MATC project. The crashes reviewed indicated that many ROR crashes exhibit similar attributes:

- Drift Off Road: vehicle slowly departs roadway (typically at a small angle of departure and straight-line trajectory). This condition is most commonly associated with drowsy or impaired drivers, or drivers with medical episodes.

- Overcorrection: the vehicle experiences a path change (drift out of lane, lane change, avoidance maneuver), then the driver overcompensates and over-steers while attempting to guide the vehicle back to the desired lane. This roadside departure type commonly results in spinout and skidding.

- Failure to Negotiate Curve: vehicle veers to the outside of a curve. Condition is frequently associated with high travel speeds or poor pavement friction (e.g., ice).

- Avoidance Maneuver: vehicle performs evasive maneuver to avoid crashing into an object, person, or animal in lane. This roadside departure condition is commonly associated with higher travel speeds (e.g., freeway), and is abrupt and panicked.

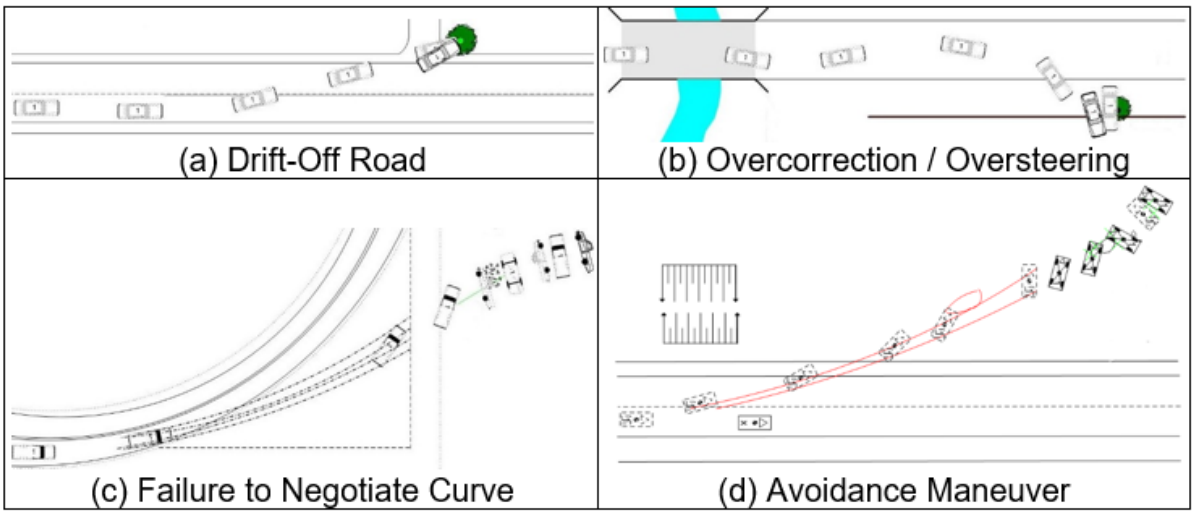

Figure 1.1 Examples of ROR Crashes (images take from NHTSA's NASS CDS)

New technology is installed in modern vehicles to help reduce the frequency of ROR excursions. Advanced driver-assistance systems (ADAS) assist the driver by identifying the geometry of the road using lane markings to help keep the driver on the road [5-7]. However these systems are subject to considerable limitations. They are not able to characterize the geometry of the roadway in all conditions, and may be affected by weather, lighting, false readings, or the lack of road markings.

1.2 Objective

1.2.1 Overall Objective

The objective of this project is to develop a vehicle-to-infrastructure (V2I) system which can assist the vehicle in remaining on the roadway.

1.2.2 Scope

This research study corresponds to Year 2 of the MATC Virtual Barrier project. The anticipated research progression for this project is shown in figure 1.2. Researchers reviewed concepts of vehicle dynamics, lane positioning, localization, and instrument operations. Road geometries, including lane centerlines, were mapped using various techniques and the geospatial orientations and guidance of each route were compared to overhead views of the routes. System flow models were generated to demonstrate the progression of data flow, and requirements for system operation. Lastly, simulation models of vehicle dynamics, driver reactions, and path corrections were generated and route correction techniques were investigated. Note that the Vehicle Dynamics Localization module was not investigated during this research phase.

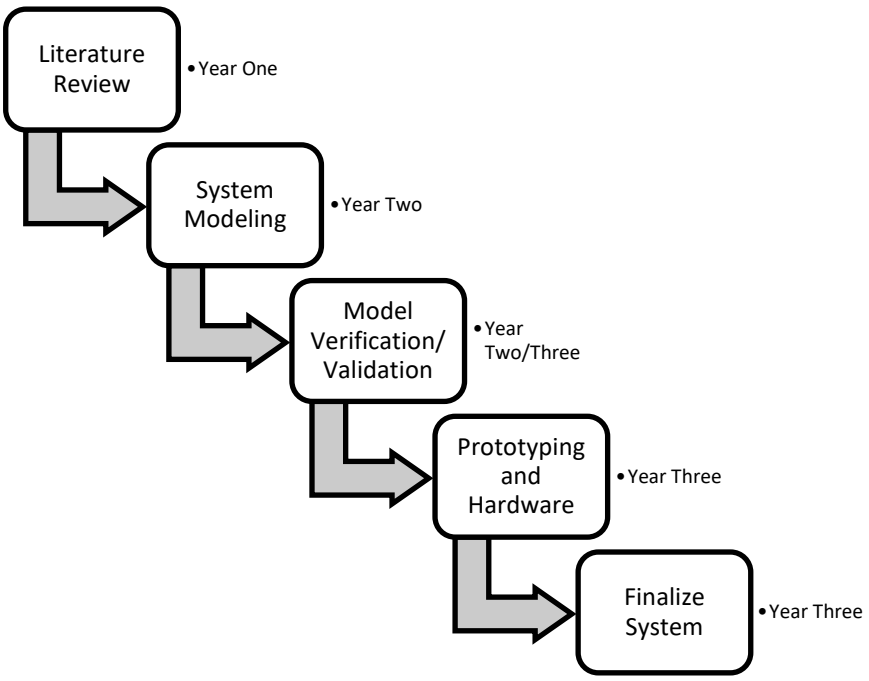

Figure 1.2 MATC Research Plan

1.3 Organization

The organization of this report focuses on explaining a new method to provide vehicle guidance utilizing V2I communication. Chapter 2 of this report offers a background section summarizing the year 1 report with major findings regarding the current state of transportation technology. After the conclusion of the background research, a new method for providing guidance parameters for autonomous technology is offered. Chapter 3 describes a basic overview of this method.

Chapter 4 describes the operation of the Lane Boundary Definition module as well as the mathematical basis for generating lane boundaries. Chapter 5 describes initial research supporting the Vehicle Path Following module. The main focus of this chapter is to offer system development strategies and a proposed system implementation that is compatible with the

methods disclosed in Chapter 4. Chapter 6 describes future research and presents an outline of steps to be executed during Year 3.

Chapter 2 Technology Review

2.1 Existing and Implemented Features

Most vehicle embedded systems which are considered as part of "intelligent transportation systems" are classified as either Advanced Driver Assistance Systems (ADAS) or Autonomous Driving Systems (ADS). Likewise, vehicles which have a high degree of onboard electronic decision systems or which utilize wireless communication, such as Vehicle-to-Vehicle (V2V), Vehicle-to-Infrastructure (V2I), or more generally Vehicle-to-Everything (V2X), are generally considered to be Connected and Autonomous Vehicles (CAVs). For the purposes of this report, vehicles equipped with onboard intelligent systems are deemed CAVs.

CAVs can be classified into different levels of autonomy based on the scope of responsibility dedicated to the vehicle computer. The SAE has published a set of autonomy levels in *SAE Recommended Practice J306 2018.* These levels of autonomy are based on the responsibility of Dynamic Driving Tasks (or DDT). DDTs can be classified into two main tasks: Longitudinal DDTs and Lateral DDTs:

- Longitudinal DDTs focuses on controlling the brake and throttle to achieve the desired forward vehicle travel behavior.
- Lateral DDTs involve maintaining the desired vehicle travel direction by modulating braking and steering that range from simple guidance on the road and evolve to avoidance for emergency maneuvering.

DDTs can be performed by either a human driver or an autonomous controller in the vehicle. The more DDT tasks that the vehicle controller is responsible is for, the higher the autonomy level. In general, for levels of autonomy 0, 1, and 2, a human driver performs all DDTs. Levels 3 and 4 provide some complete vehicle automation wherein a controller takes over certain DDTs subject to criteria (minimum speed, clear visibility, etc), and level 5 consists of full

vehicle control of all DDTs. Currently, no level 5 autonomy vehicle exists on the current market [8].

The level of autonomy and vehicle capability depends heavily on the type of sensors a vehicle has onboard. These sensors were discussed previously in [9]. A simple overview of the main sensors in a vehicle is shown in figure 2.1. These sensors can be used for two main functions: localization and environment recognition. Environment recognition can be in the form of light sensors, or ultrasound sensors. Localization sensors are usually in the form of Global Positioning Systems. All sensors work together to determine the vehicle's precise position within its travel lane. Environment recognition sensors may operate differently in different environments with outcomes affected by amount of brightness, the quality of paint in lane markings, and background information that can blend into images. Furthermore, weather disruptions have proven image recognition from light sources to be deceptive. For positioning, GPS has presented a degree of error around 6 feet which is enough to misplace a vehicle in a different lane [10].

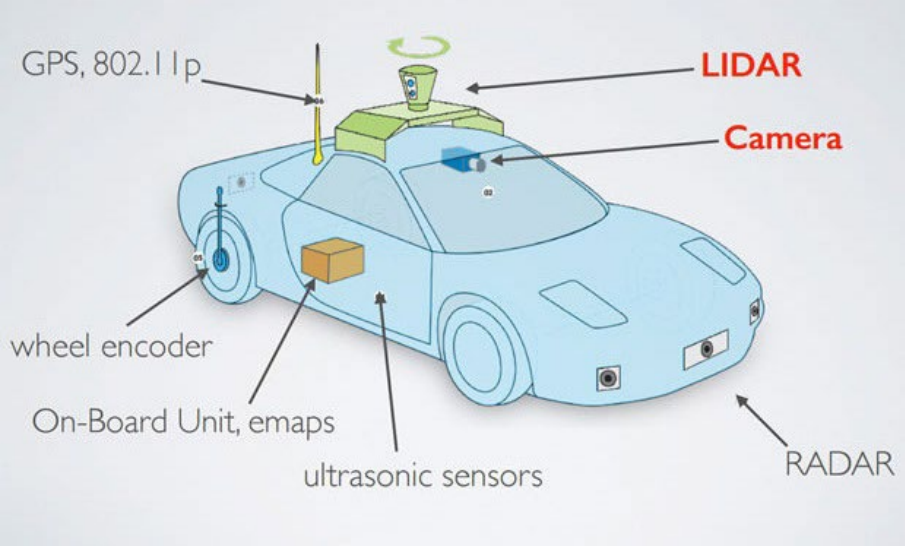

Figure 2.1 Vehicle Sensors [11]

In recent years, infrastructure has been used as a new medium for providing more information to autonomous vehicles. Specifically, V2I communication has been expanding as a new area of research in the transportation field. This technology has been used to provide traffic flow data to vehicles that comes from a station monitoring current state of traffic of a given area. As of today, this technology is still in development and being tested by Departments of Transportation (DOTs) and research agencies.

2.2 Unresolved Issues affecting Risk of Run-Off-Road Crashes

Currently, there are many areas of research that focus on developing different categories of vehicle lane-keeping technology, mainly related to vehicle sensor-based data acquisition. These features have demonstrated excellent performance under controlled environments, but many roadways differ significantly from the as-tested environments. For example, poor roadway quality or deviations between “old” and “new” roadside paint lines can create recognition problems for optic systems which rely on clearly differentiable paint edges. Adverse weather events, such as rain, snow, ice, and fog may obscure lane edges and prevent proper recognition of visual systems. Many northern states utilize salt mixtures to prevent or manage ice formation on roads during winter months, which can lead to pavement bleaching and affect lane edge identification. Most machine vision lane-keeping systems also require a minimum speed to be activated, and as such, may not function as expected when conditions are icy or traffic is heavy, and both travel speed and lane edges are largely obscured.

Alternative lane-keeping methods are still being developed. GPS-assisted systems to date have not shown sufficient accuracy to maintain vehicles in a lane and prevent them from encroaching into adjacent lanes, which could cause a crash or instability. Wirelessly connected systems which compliment GPS, such as those used by Waymo (Google) and Uber, require an extensive urban network of monitors which externally track vehicle position relative to fixed

points and would be extremely expensive to implement at the scale of modern transportation demand, and in all areas (urban, suburban, rural) and all roadways (freeways, federal highways, state highways, urban arterials, rural arterials, urban local roads, rural local roads, rural low-service roads, and private drives).

2.3 Preview of MATC Smart Barrier Solution

The MATC Smart Barrier approach considered the benefits of both local and non-local evaluation of vehicle position and the desired vehicle path using V2I. V2I communication has previously shown merit when communication equipment was used with traffic device timing and for vehicle tracking when installed adjacent to replica roadside barrier systems [6,12]. Researchers intend to build on ongoing NSF research with wireless V2I research by defining the paradigm of communication, information exchange, and road data decomposition. Moreover, the proposed system is independent of the vehicle sensors and is not affected by some of the same environmental disturbances that can adversely affect the operation of vehicle sensors.

This system is not intended to completely replace existing vehicle guidance systems as it is not meant to control or operate the vehicle. It is intended that the functionality of the system proposed and described in this report would be paired with other ADAS systems to safely accommodate random interjections (e.g. pedestrians or animals in the roadway), pre-crash braking and crash avoidance systems, blind spot warnings, and other vehicle safety systems. The main purpose of this system is to provide the necessary information to the vehicle so that it may remain safely on the roadway.

Chapter 3 Midwest Smart Barrier: Method Overview

Current sensor-based vehicle guidance and run-off-road avoidance measures are expected to improve and manage an increasing number of environmental and road conditions, but significant limitations have not yet been satisfactorily addressed. Researchers proposed an externally informed system which, when combined with the computational capabilities on the vehicle, can lead to much finer vehicle controls and a broader range of supported roads and travel conditions. The method consists of three distinct modules denoted as: Lane Boundary Definition, Dynamic Vehicle Positioning, and Vehicle Path Following.

- The Lane Boundary Definition module consists of mathematically describing a travel lane and the lane centerline, and converting lane boundaries into spatial coordinates (local Cartesian coordinates or global latitude and longitude). When lane boundaries are indeterminate (e.g., rural roads), it is anticipated that road boundaries will be used as lane boundaries. The coordinates of the lanes identified during Lane Boundary Definition module will be digitally stored on the vehicle and could be established using wireless data connection.

- The Dynamic Vehicle Positioning module will include a combination of vehicle onboard sensors and external V2I communication. Inertial measurement units (IMUs) will estimate the vehicle's instantaneous position and speed using data from instruments such as accelerations, speed, heading angle, and steer angle. Central processing units (CPUs) will predict future vehicle displacements using short-term memory of vehicle inputs. To improve the accuracy of the vehicle position estimate and prevent drift or shift accumulation, the vehicle will incrementally receive positional updates from the infrastructure and update the current position estimate as well as potential future calculated trajectories.

- The Vehicle Path Following module will consist of vehicle and/or driver inputs as reactions to the Dynamic Vehicle Positioning output. Using established thresholds for safe and controlled vehicle guidance based on the vehicle's instantaneous travel speed and brake or throttle application, the probability that the vehicle departs the road on the expected future trajectory will be identified and if a maximum risk threshold is exceeded, the driver will be warned, using audible warnings, visual cues, or tactile stimulation. Vehicles equipped with additional safety features may be able to execute avoidance maneuvers autonomously to safely guide the vehicle back to the target path and at a safe travel speed.

The proposed system and modules may provide substantial benefits to both human and autonomous vehicle navigation. This report describes the overview of the operations and

objectives of each module. Further descriptions, clarifications, development, refinement, and implementation of these systems are expected during the Year 3 execution of this project.

3.1 Objectives

The objectives for the MATC Smart Barrier are to describe the framework, operation, calculations, and system components needed for a virtual smart barrier system for keeping vehicles on the roadway. It should be noted that the MATC Smart Barrier described does not have a physical barrier component, instead utilizing electronic communication, virtual boundaries (e.g., "geofencing"), and processing systems to operate correctly. A schematic representation of the operational objectives of the Midwest Smart Barrier is shown in figure 3.1.

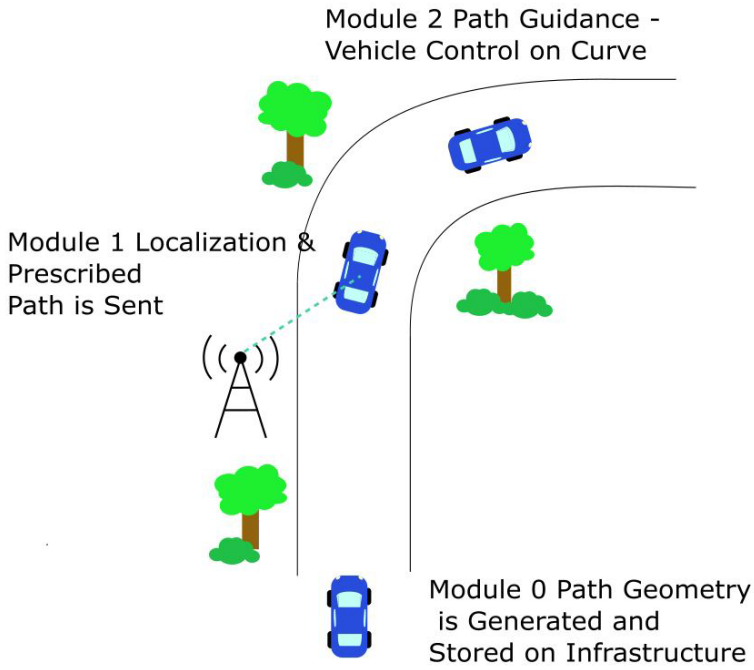

Figure 3.1 Midwest Smart Barrier Concept

3.1.1 Lane Boundary Definition Module

The objective of the Lane Boundary Definition module was to develop an accurate, verifiable representation of the road with accuracy on the order of +/- 6 in. and with reasonable precision of full-scale measurement, and which minimized the amount of data which had to be collected, stored, and transmitted to a vehicle. The data that is being transmitted to the vehicle needs to be comprehensive enough to provide necessary information so the vehicle can stay on the roadway. Additionally, the data that is transmitted cannot be cumbersome such that the data packets require a significant amount of transmission bandwidth and take time for the vehicle computer to process. The data also needs to reliable: (1) in all environmental conditions so that the vehicle can effectively navigate the roadway regardless of environmental conditions or visibility limitations; (2) with all types of vehicles, as long as they are equipped with the necessary equipment; and (3) for any roadway type, road material, and lane marking in both rural and urban areas. It is anticipated that future manifestations of this system which can be updated in real time could accommodate work zone construction areas and temporary lane closures due to emergency medical, fire, or police services.

3.1.2 Vehicle Dynamic Localization Module

The objectives of the Vehicle Dynamic Localization module were to establish a wireless connection between the vehicle and the roadside infrastructure, and identify the vehicle's instantaneous position, heading, speed, and stability. These objectives would be accomplished using several tasks. First, wireless communication would be established with dedicated transmitter-receiver pairs on the vehicle and roadside equipment, and the connection would be used to both transmit road data updates and vehicle positional information. The vehicle position may be determined either based on phase lag, signal location triangulation, reference marker identification, roadside beacon assistance, or other techniques. The target for vehicle localization

will be to have a maximum positional error calculation of 6 in. from the actual vehicle reference point (e.g., center of mass or point on vehicle centerline corresponding to front axle) with a maximum lag from instantaneous UTC-coordinated real time of 5 ms at 60 mph.

3.1.3 Vehicle Path Following Module

The objectives of the Vehicle Path Following module are to relate vehicle kinematics to the road profile, identify the nominal positional error of the vehicle from an "ideal" lane occupation, and identify what corrections, if any, are required to return the vehicle to the target path. The vehicle instantaneous positional data and road shape data obtained from the Vehicle Dynamic Localization module will be analyzed. The instantaneous vehicle position will be correlated with road data and the lateral deviation of the vehicle position from the "ideal" trajectory will be calculated, as well as deviations in speed from a target maximum speed (initially equal to the speed limit, but which could be modifiable based on weather conditions, speed limit, and work zone constraints in future iterations), vehicle heading angle and steering input, and stability (angular rates of change and instantaneous offsets from "nominal" level condition). It is anticipated that the corrections will be related to vehicle speed to increase safety and caution at high speeds, but permit greater deviation (both in terms of position and kinematics) at lower speeds. The corrections calculated by the system may be unique based on vehicle type and could be proprietary. The corrections will correlate turn radius (steering) with path curvature and trajectory estimations based on predicted deviations, occupant comfort, and vehicle performance limitations. Human driver augmentation systems will then relay correction data in the form of audible, tactile, and/or visual warnings, whereas autonomous (or semi-autonomous) systems may make automatic corrections.

3.1.4 Summary

The modules of the system are expected to perform independently. The operation of the Midwest Smart Barrier system is schematically shown in figure 3.2. A summary of the objectives of each module are shown in table 3.1.

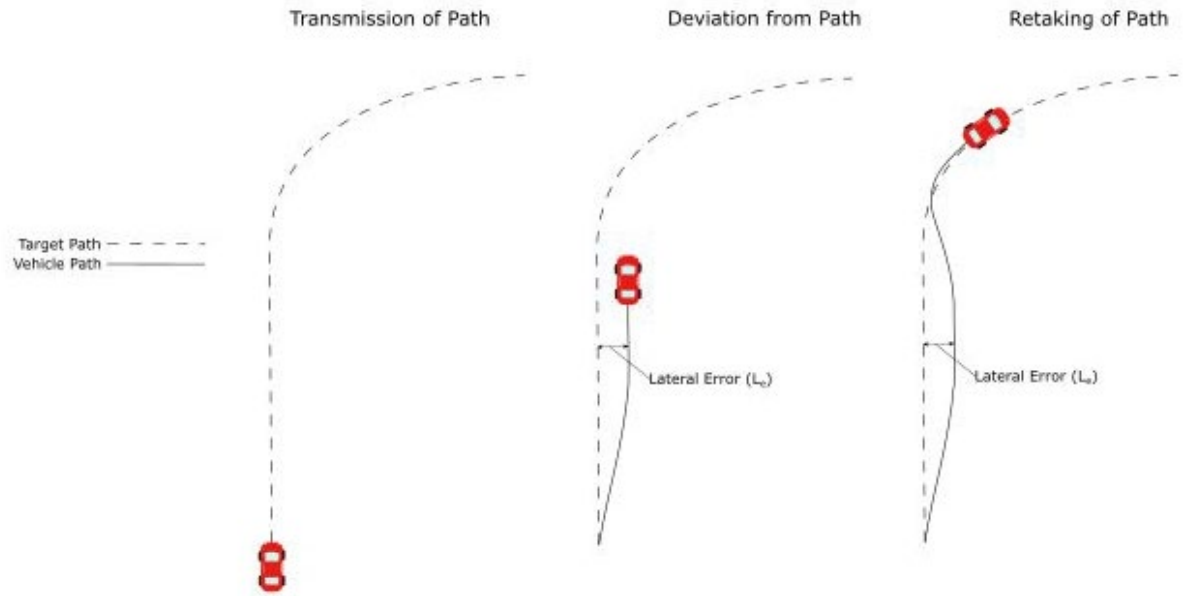

Figure 3.2 Navigation-Correction Scheme

Table 3.1 Summary of Midwest Smart Barrier Module Operations

Module	Objectives	Operation	Equipment
Lane Boundary Definition	Digitize & generate spatial & mathematical representation of lanes	Identify lane boundaries Determine boundary coordinates Calculate lane curvature Convert to data matrix	Overhead photography Lidar Survey points Crowdsourced
Dynamic Vehicle Positioning	Exchange road shape data & determine vehicle position in real time	Wirelessly relay road shape & vehicle location data Convert positional data to relate vehicle position to road geometric	Wireless radios Vehicle CPU system Other ADAS (optional)
Vehicle Path Following	Identify vehicle position relative to lane edges and determine if corrective action is required	Calculate offset current vehicle position & kinematics to "ideal" or target lane kinematics in vehicle space Compare vehicle dynamics & kinematics to vehicle stability & ROR departure thresholds Determine what corrective actions (if any) needed to keep vehicle on roadway	Vehicle CPU

3.2 Assumptions

The operation of the Midwest Smart Barrier System is assumed to satisfy the following conditions:

1) The vehicle possesses the necessary equipment and computational power to process wireless data and evaluate with ad hoc, live data collection.
    a. For manually-operated vehicles: driver alert/warning systems will be implemented to warn drivers of potential for ROR crashes
    b. For autonomous vehicles: equipment required to steer, apply throttle and brake pressure, and detect wheel slip required to correct vehicle trajectory

2) There are no random abnormalities in the road environment that would adversely affect a vehicle's trajectory along the roadway such as potholes, animals crossing, or construction zones.
    a. In-road obstruction avoidance is considered the responsibility of collision-avoidance systems (ADAS)
    b. Degenerated road elements (e.g., potholes) may compromise the quality of lane keeping system operations. Crowd-sourced data may provide information on obstructions in the roadway
3) Connectivity exists throughout the driven corridor and the operation of the wireless system.

Only the baseline operation of the Midwest Smart Barrier system is described in this research. Specifically, this report does not describe the operation of the vehicle localization module, as the design of the wireless interface and hardware were beyond the scope of this research effort. It is anticipated that additional features and capabilities of the system, including variations in safe operational speeds, diversions, lane closures (e.g., emergency services or construction work) can be added. It is anticipated that other ADAS operations including optical lane keeping assistance systems, crash avoidance systems, blind spot and cross-tracking warnings, and other features may also be used.

Chapter 4 Lane Boundary Definition Module

4.1 Mathematical Basis for Generating Trajectories

4.1.1 Background Information

In motion planning, a path is defined a set of possible ways a vehicle is allowed to travel from Point A to Point B, while trajectory is defined as the profile created by a vehicle traveling between Points A and B. For example, many trajectories can lie inside of a given path, as shown in figure 4.1. The attributes of possible trajectories are those which satisfy the mathematical requirements of the path in the form of differential constraints from equations of motion, geometrical constraints or dynamic constraints from vehicle limits.

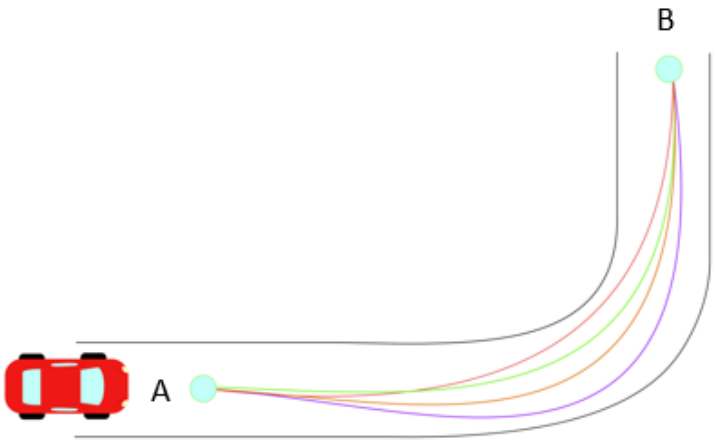

Figure 4.1 Different Trajectories in a Given Path from Point A to Point B

4.1.2 Common Methods for Trajectory Generation

In autonomous vehicles, many techniques have been used to generate trajectories traversing curves that satisfy a set of given constraints [13] [14] [15]. These techniques are mostly based from Calculus of Variations in which one or more parameters are chosen to be optimized. This can be either total length, velocity, acceleration, or a combination of factors.

These parameters are related through a functional (function of functions). Thus, most trajectory generation methods are used to optimize parameters within a functional. The most common parameter to minimize is the magnitude of the jerk (derivative of acceleration) which is related to driving comfort. This is shown by the functional:

$$F = \left(\frac{\partial^3 y}{\partial t^2}\right)^2 + \left(\frac{\partial^3 x}{\partial t^2}\right)^2 \tag{4.1}$$

Where:

x = Horizontal Position of Vehicle (m)
y = Vertical Position of Vehicle (m)
t = Time (sec)

The resulting solutions often result in fifth degree polynomials in the form:

$$x(t) = a_0 + a_1 t + a_2 t^2 + a_3 t^3 + a_4 t^4 + a_5 t^5 \tag{4.2a}$$

$$y(t) = b_0 + b_1 t + b_2 t^2 + b_3 t^3 + b_4 t^4 + b_5 t^5 \tag{4.2b}$$

Where the coefficients a_n and b_n can be found from boundary conditions existing in the starting and ending points. A complete formulation of this problem for the example of jerk minimization is offered on Section 4.2.1.1. Solving these optimization problems yields an equation known as Euler-Lagrange which often leads to fifth degree polynomials with differential constraints [16] [17]. These methods often need non-holonomic constraints that are defined as constraints on higher order derivatives of the positions (i.e. velocity and acceleration).

Other techniques involve generating clothoids (known as Euler spirals, or spiral curves) are commonly used in road design. These curves are created by doing a parametric plot of two

different Fresnel Integrals. By definition, Fresnel Integrals are trigonometric integrals that cannot be solved analytically. Often, series approximations are used for solving for Fresnel Integrals such as:

$$F_1(x) = \int_0^x \sin(t^2)\,dt = \sum_{n=0}^{\infty} \frac{(-1)^n x^{4n+3}}{(2n+1)!\,(4n+3)} \tag{4.3a}$$

$$F_2(x) = \int_0^x \cos(t^2)\,dt = \sum_{n=0}^{\infty} \frac{(-1)^n x^{4n+1}}{(2n+1)!\,(4n+1)} \tag{4.3b}$$

Because of this type of non-closed form solutions, numerical methods have to be used for the calculation of clothoids. This poses a problem because time of computation increases considerably compared to the fifth degree polynomials.

4.1.3 Euler-Lagrange General Formulation

While most trajectory and path criteria formulations result in challenging equation sets, it is often easier to find a solution to a complimentary problem and apply complimentary solutions as trajectory formulations. For these instances, Euler-Lagrange formulation permits the evaluation of permutations on a strictly controlled complimentary solution, which simplifies the formulation of problem constraints. The background of the Euler-Lagrange equations is shown below.

Find a function $y = f(x)$ *such that the functional* $F = \int_{x_1}^{x_2} F(x, y, y')dx$ *is stationary (is minimized or maximized). Along with boundary conditions of the form* $y(x_1) = y_1$ *and* $y(x_2) = y_2$.

Assuming all functions have a continuous second derivative, it is possible to state: Let $y(x)$ be a solution that makes F stationary and satisfies boundary conditions. With this, it is

possible to introduce a new variable $\beta(x)$ and let it have zero boundary conditions $\beta(x_1) = \beta(x_2) = 0$. Through this new variable $\beta(x)$, it is possible to re-write the problem in terms of a new arbitrary variable $\bar{y}(x)$, which is denoted as the variation of $y(x)$:

$$\bar{y}(x) = y(x) + \epsilon\beta(x) \tag{4.4}$$

Where:

$\bar{y}$ = Variation of Variable y, which can be a family of curves based on different boundary conditions
y = A function that makes F stationary, for example, a solution to the problem that minimizes functional F in the case of jerk
ϵ = Small variation coefficient

Through the introduction of $\bar{y}$ and $\beta(x)$, it is possible to change the problem from solving for $y(x)$ to solving for $\bar{y}(x)$. Thus, turning the problem in the following form to find a function (or family of functions) $\bar{y}$ which makes the new functional stationary: $F(\epsilon) = \int_{x_1}^{x_2} F(x, \bar{y}, \bar{y}')\ dx$.

Given that equation (6.1) makes $\bar{y}$ dependent on x, the integral of $F(\epsilon) = \int_{x_1}^{x_2} F(x, \bar{y}, \bar{y}')\ dx$ will provide a functional $F(\epsilon)$ that only depends on ϵ. For this reason, it is possible to make an optimization problem with simply the derivative of the functional F with respect to ϵ:

$$\frac{dF}{d\epsilon} = 0 \tag{4.5}$$

In optimization problems, it is necessary to evaluate the function (or functional) at an extrema point. For this situation, ϵ can be evaluated at zero, which will provide an extrema as follows:

$$\bar{y}(x) = y(x) + \epsilon\beta(x) \;\rightarrow\quad \bar{y}(x) = y(x) \tag{4.6}$$

Provided the assumption of $y(x)$ is a solution that makes F is stationary. By setting ϵ to zero, the functional F can be optimized.

$$\left.\frac{dF}{d\epsilon}\right|_{\epsilon=0} = 0 \tag{4.7a}$$

To evaluate this optimization problem, the definition of F is used which gives an integral equation to solve:

$$\left.\frac{d}{d\epsilon}\right|_{\epsilon=0} \int_{x_1}^{x_2} F(x, \bar{y}, \bar{y}')\, dx = 0 \tag{4.7b}$$

$$\int_{x_1}^{x_2} \left.\frac{d}{d\epsilon} F(x, \bar{y}, \bar{y}')\, dx\right|_{\epsilon=0} dx = 0 \tag{4.7c}$$

The previous integral-differential equation is solved which provides the following function:

$$\int_{x_1}^{x_2} \left[\frac{\partial F}{\partial y} - \frac{d}{dx}\frac{\partial F}{\partial y'}\right] \epsilon\, dx = 0 \tag{4.7d}$$

This final equation is a product in between an arbitrary parameter ϵ and a functional. Therefore, for the previous equation to be true for any arbitrary ϵ. The following has to be true:

$$\left[\frac{\partial F}{\partial y} - \frac{d}{dx}\frac{\partial F}{\partial y'}\right] = 0 \tag{4.7e}$$

Therefore: If $y(x)$ makes F stationary, then $y(x)$ must satisfy the previous equation known as the Euler-Lagrange Equation. The details of the steps to obtain the Euler-Lagrange Equation are provided in Appendix A, along with validation of how the variation $\bar{y}(x)$ satisfies the same boundary conditions as $y(x)$, which allows to use the variation as a valid solution approach.

4.2 Trajectory Criteria

From literature review, the following criteria was selected to generate a path that solves the problem statement. The path generated needs to be:

- Able to provide a smooth ride for vehicle occupants;
  - Both the acceleration (which is related to vehicle stability and tire-pavement friction force generation) and jerk (rate of change of acceleration) are controlled.
  - From AASHTO guidelines, parameters for a smooth ride:
    - Lateral Acceleration: 0.4 to 1.3 m/s^2 (0.04 to 0.13 g's)
    - Jerk Values: 0.3-0.9 m/s^3

- Considered for compatibility with different vehicles;
  - For example, the dynamics experienced by a vehicle undergoing this path, needs to be appropriate for different vehicle sizes and types.
  - From AASHTO guidelines, overall vehicle lengths:
    - Passenger Car: 19.0 feet
    - Single Truck: 30-39.5 feet
    - Buses: 40.5-60 feet
    - Combination Trucks: 45.5-114 feet
    - Recreational Vehicles: 30-53 feet

- And accurately describes boundaries of the lane (path) and can be mapped to fixed-reference geospatial road data.

By developing this method, the outcome is expected to create a vehicle ride that is independent of:

- Road type
    - This provides independence on whether the road has pavement or road markings.
- Infrastructure signs
    - Which gives a backup to image recognition software and machine learning/neural network techniques.

- Weather conditions
    - This provides a backup to camera sensors or a lidar sensor which tend to fail on detection under different weather adversities.

Similarly, it is desired that the method is general enough to be compatible with other vehicles for future applications. The techniques cited before [13-20] are able to satisfy some of the criteria stated above. However, other methods, such as the polynomial lane approximations, are extremely sensitive to variations in coefficients of polynomial expressions, are not consistent nor map-able to GIS data (note, latitude and longitude are represented in angular formats correlated with a spherical earth coordinate system. Whereas local polynomial approximations connect consecutive geospatial points using principally Cartesian planar topological assumptions), and may be too computationally costly or poorly conditioned for real-time estimation and warning of lane departure. Researchers therefore desired a more compact method of representing roadways which could both be wirelessly transmitted to the vehicle and rapidly evaluated by vehicle onboard systems, and which was conducive for both geospatial and surface topological representations.

Researchers therefore reviewed aspects of path representation, vehicle dynamics, and coordinate transformations in an attempt to simplify the representation of the road data. These were used to compare methods of path generation and develop a proposed solution. These parameters include:

- Computation time in processing, collection, and digital transfer (communication)

- Size of data representation per unit area of collection (e.g., MB per km of road)
- Discretization intervals (e.g., length of road section between consecutive data points)
- Error accumulation and data accuracy (i.e., sensitivity to data precision)
- Vehicle dynamic constraints such as maximum acceleration and velocity
- Geometric constraints such as curvature and road geometry

From comparing techniques, it was noted how most boundary value problems such as [16] [17] offer solutions of analytical higher order equations, while others contain non-closed forms [14]. Consequently, high computation costs are needed to calculate trajectories during onboard operations. Solutions compared include coordinate and curvature polynomials of high order. These type of polynomial solutions introduce rounding and truncation errors that typically occur in machine operations [21] [22]. In autonomous vehicle operations, both accuracy and speed are essential for optimum performance. As accuracy of polynomial approximations increase by extending the operations of polynomial coefficients, its speed of transmission decreases. Decreasing the amount of coefficients provides non-compliant solutions, and the sensitivity of the coefficients is affected as well. This makes accuracy and speed of transmission an inverse relationship, which is not optimal for this V2I technology.

Therefore, it was an objective that the data transmission be optimized between use, accuracy, and computational expense for transmitting and receiving data.

4.3 Coordinate Reference Frames

Researchers desired to represent road corridor data (i.e., lane boundaries) using simple, reliable, accurate, and precise formulation. Several coordinate system representations were considered when developing a simplified road database system. A summary and discussion of those coordinate systems is presented below.

4.3.1 Cartesian Coordinates

The most common scientific and mathematical formulation for coordinates is the Cartesian or X-Y-Z coordinate system. In Cartesian coordinates, displacements are denoted as a set of orthogonal displacements along unit vectors *i*, *j*, and *k* corresponding to the X, Y, and Z directions, respectively.

It is anticipated that the lane shapes and boundaries can be approximated using a series of discrete, simple functions instead of complicated functions to describe long segments. However, these road functions must be contiguous at end points and differentiable through the second derivative, and preferred, the 3rd derivative (to allow smooth transitions in acceleration or minimized "jerk"). For local displacements and short-term projection, Cartesian space may be effective, but connecting many adjacent road segments together to generate a road network across a country such as the U.S. would have to be performed using one of two methods:

- Database of all road shapes & discrete reference positions extracted from GIS data (requires extremely-high precision road coordinates and shape functions) tabulated in X,Y, and Z coordinates; or
- Database of reference GPS positions and locally forecasted road shape functions (which due to small differences in numerical calculations, could lead to singularities at transitions between adjacent road segments).

To represent the road paths, a poorly conditioned Cartesian system may be required. For example, using a Cartesian coordinate origin at the center of the earth, road segments measuring approximately 100 ft long would have base coordinates of approximately 20,908 ft (earth radius of 3,960 miles) multiplied by both polar and azimuthal angular corrections. These corrections Include altitude changes across a road segment of inches (±0.1 ft) and using lane shape functions with coefficients controlled at sub-inch precision. While some innovative methods may be used to improve the poor conditioning of a Cartesian system, such as a dual- or conversion-based

Cartesian-to-spherical coordinate system, Cartesian coordinates were considered less desirable than other methods of representing road and lane shape boundaries.

4.3.2 Spherical Coordinate System

Current methods of triangulating earth position using the Global Navigation Satellite System (GNSS) utilize spherical coordinate systems in the form of latitude and longitude. The GNSS system describes any satellite configuration, which is used to triangulate a location on the earth. The most common GNSS system in the United States is the Global Positioning System (GPS), but additional reference frames exist, including GLONASS (Russia) and GALILEO (European Union).

The spherical reference frame denotes a fixed reference point (center) and coordinates are described in terms of three unit vectors:

- a radius unit vector, $\hat{r}$, which points in the direction of the radius from the reference point to the coordinate origin (the center of the earth);
- an azimuthal angle $\hat{\theta}$, or "longitude", which describes the angular position around the circumference of the earth from a reference position (the Greenwich or "Prime" Meridian); and
- a polar or zenith angle, $\hat{\varphi}$, or latitude, which describes the angular offset from the equator toward either the upper ("north") or lower ("south") pole.

The spherical coordinate system is denoted schematically in figure 4.2.

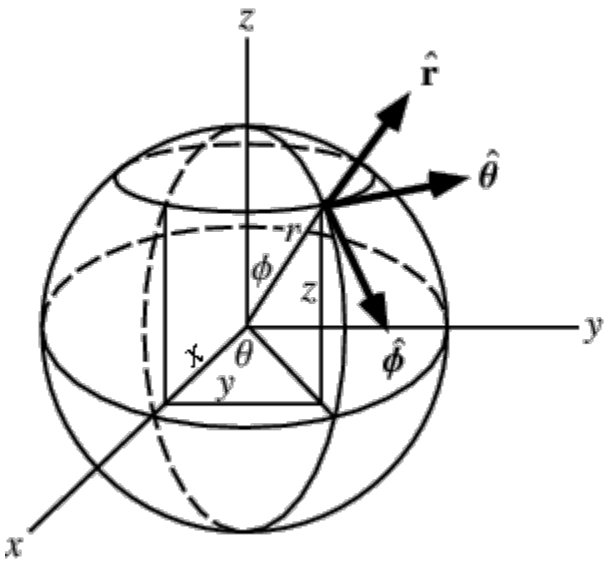

Figure 4.2 Spherical Coordinate System [23]

Due to compatibility with common GNSS triangulation systems, spherical coordinates are highly advantageous for identifying discrete locations on the earth's surface. However, representing road and lane coordinates using spherical coordinates suffer some similar challenges as the Cartesian system. Angular measurements in GNSS systems are commonly recorded in decimal radians, but a very high degree of precision is required to denote a position. For example, the MwRSF research headquarters, which houses the authors of this research study, is located at (40.821726° lon, -96.689624° lat). Using an approximate earth radius of 3,960 mi = 20,908 ft, the angular precision required to be accurate to within 0.5 ft, which is the objective for representing road coordinates accurately, is (±0.000003806° lat) or (±0.000005030° lon). The reason for the disparity between latitude and longitude precision is that the effective circumference at the 40.82 latitude is reduced by 25%.

Figure 4.3 MwRSF Design Headquarters [24]

Some techniques have been identified to improve accuracy of road boundary definition in association with tools such as Google Maps (e.g., Waymo), Apple Maps, Garmin, and other similar software and APIs of position triangulation. One such tools is the use of polylines, which is employed by Google to simplify the road representation [25]. Nonetheless, to describe lane boundaries accurately, lane boundaries would have to be mapped to spherical coordinates and combinations of local equations and global "anchor points" would need to be used along the lane. The accuracy of coefficients required for the accurate identification of lane boundaries for use in vehicle position verification would be extremely detailed and precision errors are likely to occur.

4.3.3 Normal-Tangential (Serret-Frenet)

Some coordinate systems, such as the *Serret-Frenet* or Normal-Tangential (N-T) Coordinates, are almost purely local and rely on a secondary reference system to denote position. N-T coordinates have been used extensively in works that define curvilinear motion of particles

in space [26]. For this project, a 2D Euclidean space is selected in which N-T coordinates will be used to represent the motion of a vehicle's center of mass traversing a curve as shown in figure 4.4.

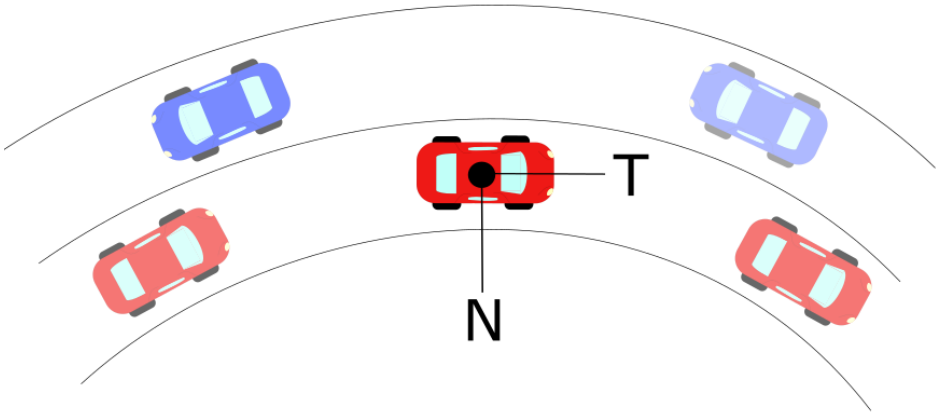

Figure 4.4 Normal-Tangential Coordinates along a Curve

As the vehicle goes through the curve, it is limited to constraints provided by road geometry and friction limits on the vehicle tires [27] [28]. These limits are related to the acceleration a vehicle goes under circular motion, which is denoted as:

$$a = \dot{v}\,T + \kappa v^2\,N \tag{4.8}$$

Where:

a = Total Acceleration of Vehicle (m/s2)
v = Tangential Velocity of Vehicle (m/s)
κ = Curvature at an Instantaneous Point (m^{-1})
N =Normal Unit Vector
T= Tangential Unit Vector

Curvature can be defined analytically, physically and geometrically. It measures how fast the tangential unit vector T changes with respect to a differential change in position along a

curve. The inverse of curvature is known as radius of curvature, ρ, which corresponds to the radius of circumscribed circle which is tangent to, and describes, the path at a point in a curve. By definition of N-T coordinates, a vector perpendicular to the curvature direction will provide a velocity tangent vector approximation. This velocity vector provides a heading angle to the desired trajectory that is needed to follow a road path.

This curvature can be expressed in a vector form that has a direction in the Normal Unit Vector shown in figure 1.2. Derivations for defining curvature have been extensively developed in other works [26] [27]. Curvature is a tremendously advantageous method of representing road boundaries due to simplicity, compatibility with vehicle dynamics (meaning it is intrinsically related to vehicle stability from spin-out or skid-out and performance limits), and compatibility with global measurement systems.

4.4 Application of Normal-Tangential Coordinates to Road Boundary Mapping

Researchers concluded that the most advantageous method of representing lane boundaries was to use local road coordinates, expressed in terms of curvatures and distances, and map those to an external reference frame such as the spherical coordinate system for compatibility with GNSS systems. The proposed method of generating lane boundaries required the determination of curvatures of each lane segment in local space, the parameters describing the geometry of those lane boundaries, and the anchoring of those boundaries to geocentric spherical space using anchor points. The derivation of interest is explained in detail below.

4.4.1 Discrete Curvature Formulation

Let a scalene triangle with corners A, B, and C have a circumscribed circle of radius R in Euclidean 2D space as shown in figure 4.5.

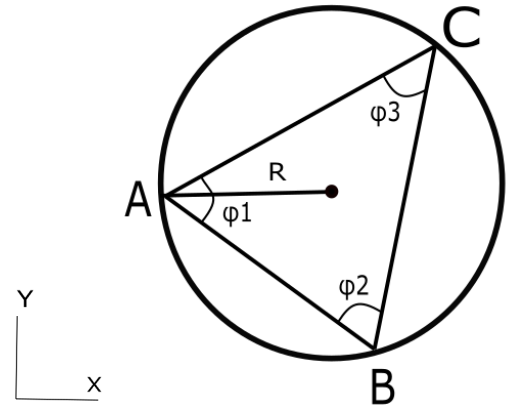

Figure 4.5 Circumscribed Circle in Scalene Triangle

If we let a vector D be the cross product in between the vectors AB and AC, the direction will be pointing out normal to the plane defined by the intersection of AB and AC. By definition of the magnitude for cross product:

$$\|D\| = \|AB \times AC\| = \|AB\| \|AC\| \sin\phi_1 \tag{4.9}$$

Let vector E be the cross product of D with the vector AB, defining this new vector in the direction of e_1 as shown in figure 4.6. Let the magnitude of vector E be defined as:

$$\|E\| = \|D \times AB\| = \|AB\|^2 \|AC\| \sin\phi_1 \tag{4.10}$$

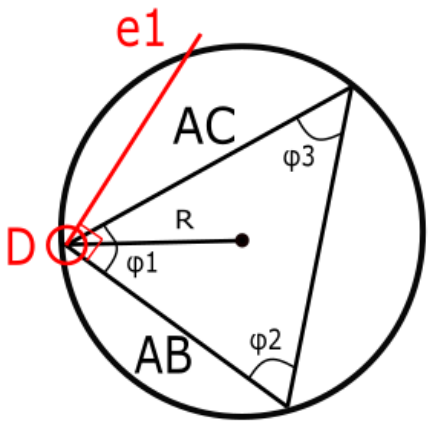

Figure 4.6 Circumscribed Circle with Unit Vector $\boldsymbol{e_1}$

Similarly, let a vector F be the cross product of D with the vector AC, defining this new vector in the direction of e_2 as shown in figure 4.7. Let the magnitude of vector E be defined as:

$$\|F\| = \|D \times AC\| = \|AB\|\|AC\|^2 \sin\phi_1 \tag{4.11}$$

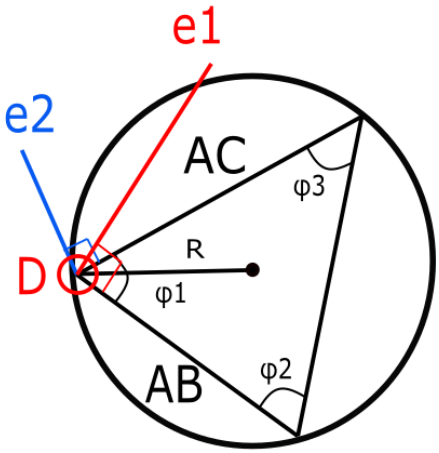

Figure 4.7 Circumscribed Circle with Unit Vectors $\boldsymbol{e_1}$ and $\boldsymbol{e_2}$

The unit vectors of e_1 and e_2 are defined by the following:

$$e_1 = \frac{E}{\|AB\|^2 \|AC\| \sin \phi_1} \tag{4.12a}$$

$$e_2 = \frac{F}{\|AB\| \|AC\|^2 \sin \phi_1} \tag{4.12b}$$

By definition, the midsection of any triangle's side intersects with each other at a point P as shown in figure 4.7. These intersecting lines denote two triangles with the same angle ϕ_1 in between the unit vectors and their corresponding midsections as shown in figure 4.8 below.

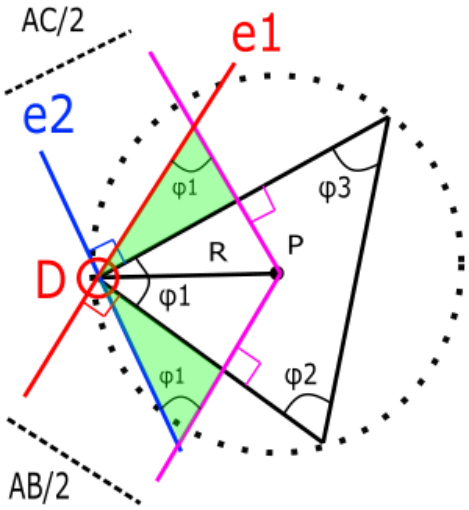

Figure 4.8 Triangles Formed through Intersections of Unit Vectors

From these triangles, the components of vector DP along unit vectors e_1 and e_2 can be obtained:

$$DP_1 = \frac{AC}{2 \sin \phi_1} \; e_1 = \frac{E}{2\|AB\|^2 \sin^2 \phi_1} \tag{4.13a}$$

$$DP_2 = \frac{-AB}{2\sin\phi_1}\, e_2 = \frac{-F}{2\|AC\|^2 \sin^2\phi_1} \tag{4.13b}$$

From our previous definition of the vector D, it is possible to simplify further:

$$DP_1 = \frac{\|AC\|^2 E}{2\|D\|^2} \tag{4.13c}$$

$$DP_2 = \frac{-\|AB\|^2 F}{2\|D\|^2} \tag{4.13d}$$

With these components, it is possible to obtain the full vector as the sum of the components:

$$DP = \frac{\|AC\|^2 E}{2\|D\|^2} - \frac{\|AB\|^2 F}{2\|D\|^2} \tag{4.13e}$$

$$R = \frac{\|AC\|^2 E - \|AB\|^2 F}{2\|D\|^2} \tag{4.13f}$$

Using previous definitions of E and F:

$$R = \frac{\|AC\|^2 \|D \times AB\| - \|AB\|^2 \|D \times AC\|}{2\|D\|^2} \tag{4.13g}$$

Using previous definition of D, it is possible to obtain the radius of the prescribed circle in terms of only the difference in between points A, B, and C.

$$R = \frac{\|AC\|^2\|(AB \times AC) \times AB\| - \|AB\|^2\|(AB \times AC) \times AC\|}{2\|(AB \times AC)\|^2} \tag{4.13h}$$

Using the previous definition, it is possible to apply the formulation of R to differentially small arc segments as it is shown in figure 4.9.

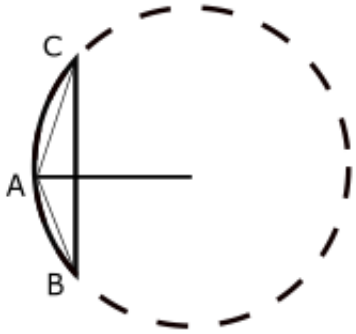

Figure 4.9 Scalene Triangle in Arc-Segment

By definition, the radius of this circumscribed circle is called radius of curvature, and its inverse is known as curvature denoted as:

$$\kappa = \frac{1}{R} \tag{4.14}$$

Through this definition, it is possible to extend the application of this discrete radius of curvature and applying it to long-discrete arc segments as shown in figure 4.10 below.

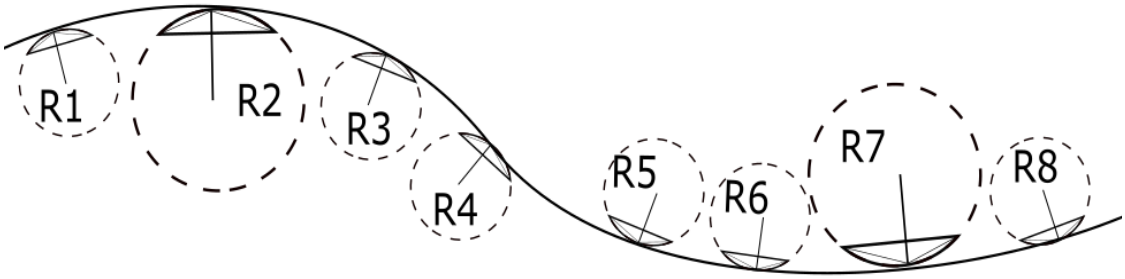

Figure 4.10 Road Section with Discrete Sections

It should be noted that in the special case that points A, B, and C are collinear, the curvature is by definition equal to zero, and the radius of curvature is therefore theoretically infinite. However, allowing curvature to be directional along the principal travel direction of the roadway, it is therefore possible to use a continuous variation of curvature throughout a lane segment without instabilities or singularities which could be encountered during tangent road segments.

Based on this method, it is possible to obtain curvature vectors at discrete sections of any given lane. With these vectors, the heading angle can be calculated through two different approaches. The first method comes from numerical integration and the second one from an orthogonal phase shift.

4.4.2 Heading Angle Integration Formulation

The arc-length s of a curve is defined as the length traveled by a certain amount of degrees θ along a constant radius r. If s is sufficiently small, a triangle can be formed in between these three parameters, which are related through geometry:

$$\sin\theta = \frac{s}{r} \tag{4.15a}$$

Defining r as the radius of curvature at the specific arc-length and letting $r = \rho$.

$$\sin\theta = \frac{s}{\rho} \tag{4.15b}$$

By the previous assumption of small angles:

$$\sin\theta = \theta \tag{4.15c}$$

Which leads to

$$\theta = \frac{s}{\rho} \tag{4.15d}$$

Let the Curvature κ be denoted as

$$\rho = 1/\kappa \tag{4.15e}$$

Substituting this definition into equation (4.15d)

$$\theta = \kappa s \tag{4.15f}$$

Assuming a differential section for θ and s. Rearranging for κ:

$$\kappa = \frac{d\theta}{ds} \tag{4.15g}$$

By separation of variables and integration

$$\int \kappa ds = \int d\theta \tag{4.15h}$$

Which concludes that the angle of orientation as a function of arc-length s can be found through numerical integration of the curvature as:

$$\theta(s) = \int \kappa(s) ds \tag{4.15i}$$

To obtain the curvature, let a scalene triangle with corners A, B, and C have a circumscribed circle of radius r.

4.4.3 Heading Angle Orthogonal Shift

From figures 4.8 and 4.10, it is possible to notice that N-T coordinates offer collinearity in between the normal unit tangent vector and the curvature vector for any given curved road. Given this, it is possible to obtain a base heading angle that involves an orthogonal shift to the curvature vector.

This shifted curvature vector is collinear with the heading angle as along as the vehicle follows the same curvature that the physical road has. Typical highway roads are designed based on AASHTO guidelines to provide a natural, easy-to-follow path for drivers, such that the lateral force increases and decreases gradually as the vehicle enters and leaves a circular curve [31]. This leads to an approach of curvature generation based on AASHTO road geometry to obtain heading angles. To develop this, the aforementioned definition of radius of curvature is used to obtain both its magnitude and direction [32]. The radius of curvature is computed from discrete points that represent coordinates of a road.

4.5 Road Slicing

Researchers observed that the N-T coordinate system was useful for mathematically describing lane boundaries locally, and could be combined with global reference points to evaluate vehicle position against the road boundary dynamically. Therefore, the next step was to develop a method of parsing lane profiles into segments and confirming that the curvature calculation techniques could adequately describe the lane boundaries. This method was deemed "road slicing".

The road slicing method utilizes lane boundary data. This data can come in the form of different sources such as digital maps, design guidelines, lidar scans, or GPS measurements. From this data, it is possible to apply the mathematical formulae from sections 4.4.1 and 4.4.2 to obtain a road segment along with its heading angle direction. In order to explore the effectives of road slicing, different methods to coordinates were used. The first method involved a base model of the road based on AASHTO design guidelines. The second method involved using Google Earth coordinates. The third method involved using GPS coordinates.

4.5.1 AASHTO Base Model

Before evaluating actual road boundaries, researchers first investigated whether roads constructed consistently with the AASHTO "Green Book" [31] would be accurately represented using a parsed curvature model. Researchers generated a sample roadway using AASHTO Green Book techniques which was consistent with a banked turn on a freeway with a design speed of 60 mph. The sample road consisted of 5 different sections that can be classified as: tangent section, entrance transition, constant radius curve, exit transition and tangent section. Applying the discrete geometric approach to this curve, curvature vectors were plotted with respect to the road segments as shown in figure 4.11. The curvature vectors were plotted with respect to road segments to obtain a base curvature profile as shown in figure 4.12.

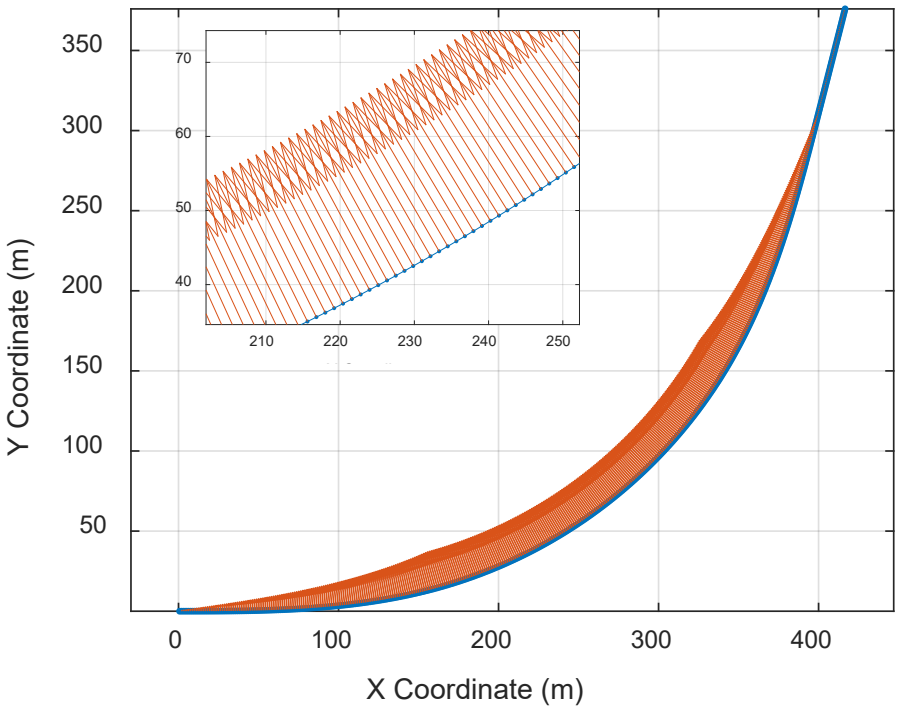

Figure 4.11 AASHTO Base Model: Road with Curvature Vectors

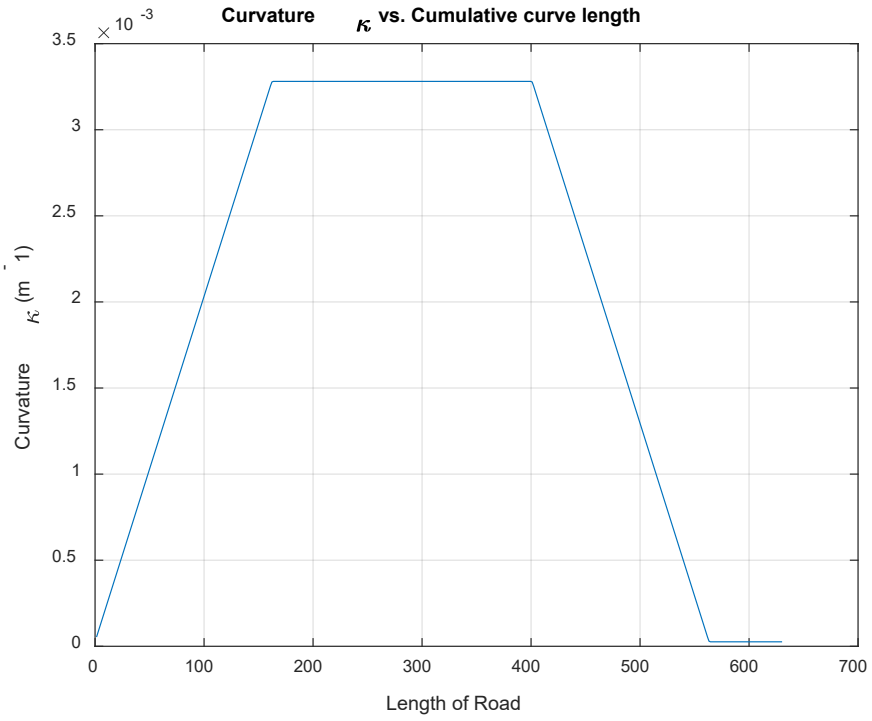

Figure 4.12 AASHTO Base Model: Curvature κ vs. Cumulative Curve Length

Results of the curvature decomposition were compelling. Although the curvature was calculated in multiple, small, discrete increments, the resulting profile of the curvature plotted as a function or longitudinal distance along the road produced a piecewise linear curvature distribution in which the transitional regions had a linearly-varying curvature and the constant-radius curve was accurately represented by the constant curvature. Likewise, the tangent section was accurately represented by a curvature of zero.

The heading angle change for the road segments were also noted. The first method involved obtaining the heading angle from the Discrete Curvature Formulation and add an orthogonal phase shift. The second method involved using the Heading Angle Integration Formulation which has been explored in different studies [e.g. 13]. The results of both methods are shown in figures 3.1 and 4.14. These resulting angles were used as input data on a controller developed in Chapter 6.

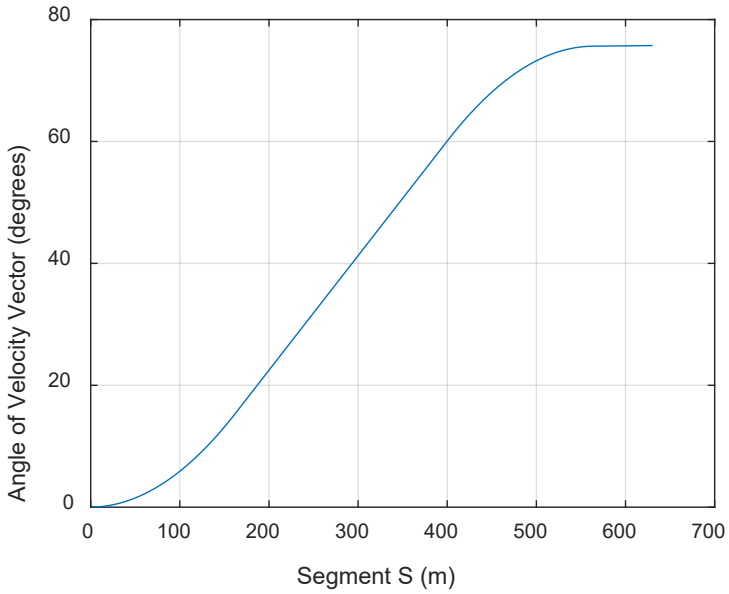

Figure 4.13 AASHTO Base Model: Orthogonal Phase Shift Approach

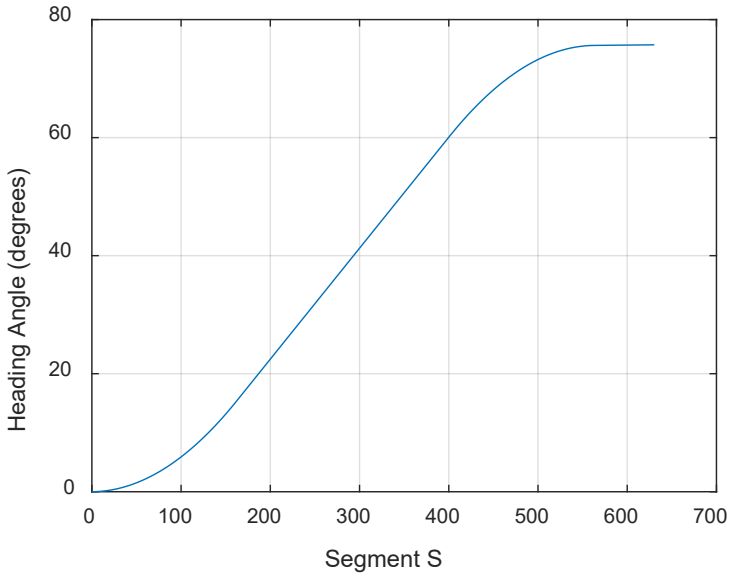

Figure 4.14 AASHTO Base Model: Numerical Integration Approach

Using an orthogonal shift from the curvature vectors, researchers plotted the velocity vectors of the sample road profile on top of the actual road shape. The velocity vectors created a highly-accurate representation of the road and instantaneous tangent vectors, indicating good agreement between numerical calculations and the sample road. Results on heading angles with respect to road segments are shown in figure 4.15.

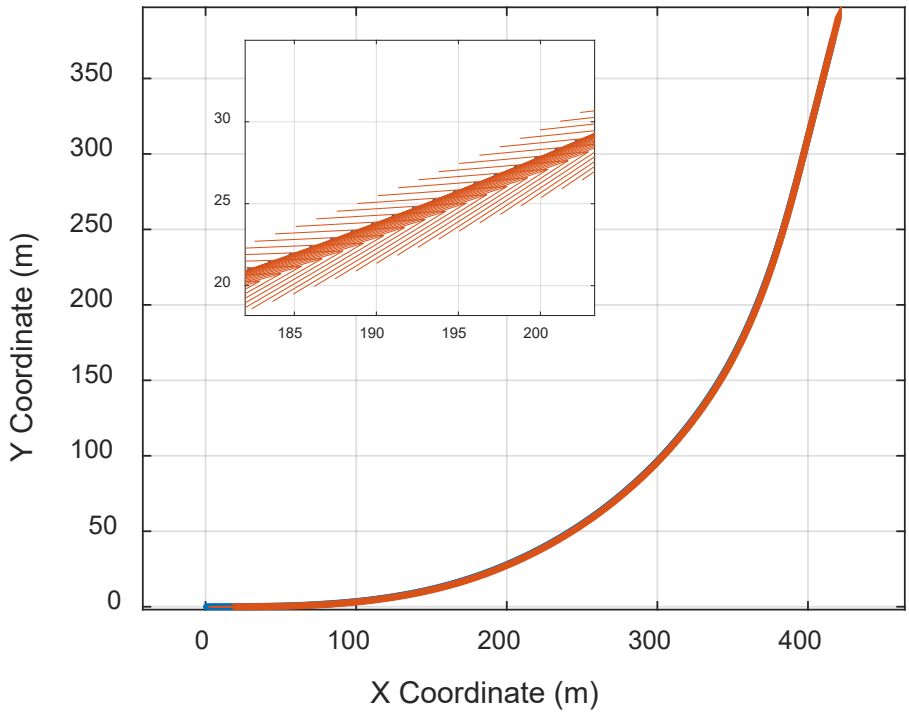

Figure 4.15 AASHTO Base Model: Road with Velocity Vectors

4.5.2 Google Earth Model

This model is based off a selection of points in Google Earth that represent a highway road with design speed of 60 mph. The points were narrowly-spaced and highly-discretized along the lane centerline. The road profile and resulting vectors from applying the discrete geometry approach are shown in figure 4.16. It is noticeable how the vector directions were subjected to noise due to the large number of samples and the small deviations per sample. The curvature magnitude with respect to length was also plotted in figure 4.17 and it was observed that magnitude deviations increased considerably compared to the ideal AASHTO model.

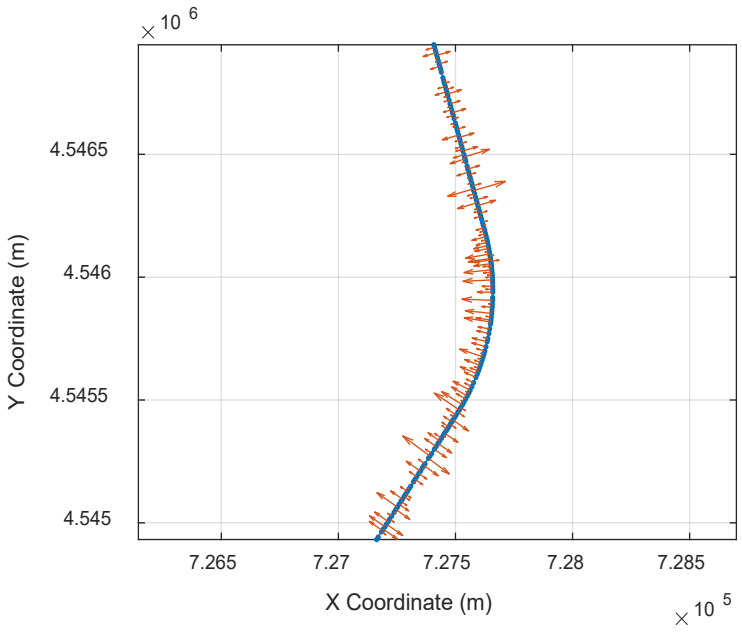

Figure 4.16 Google Earth Model: Road with Curvature Vectors

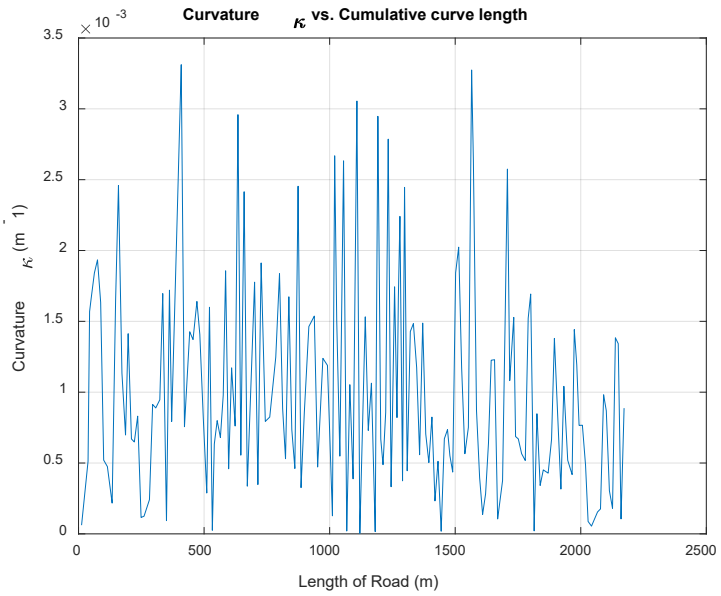

Figure 4.17 Google Earth Model: Curvature κ vs. Cumulative Curve Length

The very narrow discretization of the sample points on the roadway was intentional to evaluate the susceptibility of the road slicing to noise from numerical imperfections. Results

indicated that noise may be a concern, but the general trend of the roadway was clearly denoted. Next, the direction of the heading angle was obtained from the orthogonal phase shift still provided comparable results to those found by calculating with AASHTO as shown in figure 4.18. Similarly, the resulting velocity vectors to guide the vehicle provide a suitable heading direction as shown in figure 4.19.

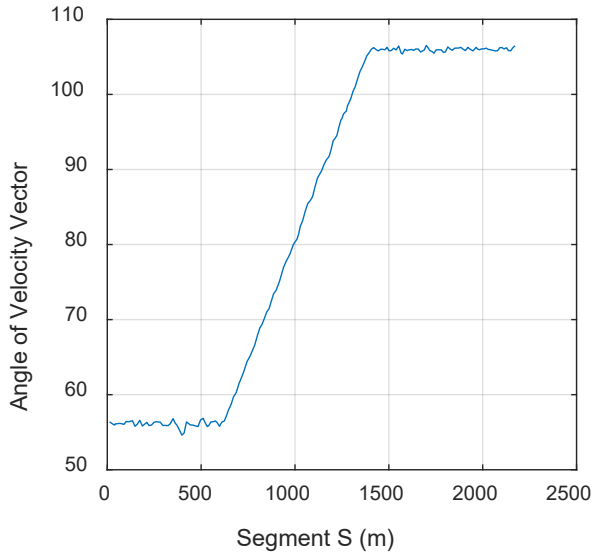

Figure 4.18 Google Earth Model: Orthogonal Phase Shift Approach

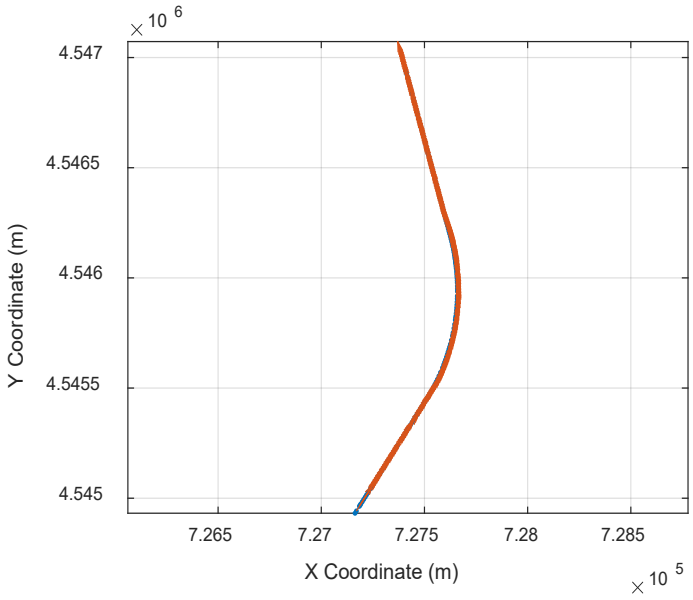

Figure 4.19 Google Earth Model: Road with Velocity Vectors

4.6 Summary and Discussion

Researchers reviewed coordinate systems and evaluated road discretization techniques. Using a combination of Normal-Tangential (N-T) coordinates combined with GPS point data, and a road curvature decomposition technique, researchers demonstrated that lane boundaries can be reasonably described, and the lane heading can be accurately identified. The combination of these techniques may produce a powerful technique for accurately representing road data with simplicity and efficiency.

More research remains to apply the road slicing and representation techniques into a database format which will allow vehicles to dynamically reference lane data and current vehicle position. However, researchers believe the foundations established in the MATC Year 2 research will provide a clear blueprint for applying these techniques to map road data in a larger scale.

Chapter 5 Vehicle Dynamic Localization Module

Researchers did not investigate the wireless communication required to perform the dynamic vehicle localization during MATC Year 2. Nonetheless, researchers identified critical parameters to apply to the localization module as targets during Year 3 and future extensions of this research. The three objectives of the dynamic localization were: (1) optimize the transmission of lane (road) data to allow rapid updates of onboard vehicle reference systems; (2) ensure the broadcast of wireless vehicle data extends throughout the road network which is covered by each transmitter; and (3) optimizing the balance of user privacy and data security to protect the users of the safety system without compromising individual 4th or 5th Amendment rights.

Further objectives were identified and summarized below.

- The transmission infrastructure will triangulate the vehicle position when needed, to provide in-lane accuracy to the vehicles to keep it securely on the road, and help to correct in-vehicle estimation and prediction techniques.
- The localization module transmission should be capable of transmitting the road data in an optimized format and accurately send the data to every vehicle on the road.
- Data transmission needs to also work in all environmental conditions (e.g., rain, snow, wind, blowing dust or debris, etc.) and throughout the coverage area from each transmitter.
- Connection speeds and data exchange should be faster than the need for the data is generated (i.e., data forecasting for future path prediction and reaction).
- The desire is to minimize the amount of transmission, receiver, and processing hardware required on the vehicle and in the infrastructure to ensure optimized cost-effectiveness. Because some funding for the transmission and data exchange may be public (government-sponsored) and some may be private, the optimization will consider both range of transmissions and connections and the cost of the transmission hardware.
- The infrastructure also needs to be able to be secured against false data and interference from people who desire to disrupt the system.

Further research on the transmission and dynamic localization module is anticipated during MATC Year 3.

Chapter 6 Vehicle Path Following Module

6.1 Problem Statement

In order to determine if the local path generation method is viable, a vehicle control structure needs to be developed that is based on the local path data. The control system needs to accurately keep the vehicle on the road, by means of driver alters or direct vehicle control.

6.2 Introduction

Driver assistance and autonomous vehicle control technologies are new and developing in the automotive industry. Advanced driver assistance systems (ADAS) are systems that are available in most new vehicles on the market, however, their range of capabilities depends on the specific vehicle model. The goal of ADAS is to use a suite of sensors in and around the vehicle to monitor the environment to detect if there is anything that will endanger the vehicle occupants and alert the driver to take corrective action or by taking direct control of the vehicle. These hazards can include other vehicles, pedestrians, wildlife, and lane departure. Autonomous vehicle (AV) technology is a level above ADAS as it seeks to be in control of the vehicle at all times and uses additional sensors in comparison. AVs are still in the prototype and development phase and are operated under the guidance of a team of experts and are constantly monitored and never allowed to be fully self-sufficient as is the end goal.

As previously mentioned, both of these systems are reliant on a suite of external sensors. The sensors interpret the environment and the onboard computer processes the information to determine what actions are necessary. These sensors are accurate in controlled environments, however, on the roadway they are affected by a variety of variables. This can be related to inclement weather that obstruct the sensors' view, other electrical signals in the environment, poor roadway labeling, and complex road geometry like sharp curves and hills [38-43]. This method of road data collection creates a problem for controlling the vehicle correctly at all times

and in all scenarios as vehicle sensors can obstructed or just interpret environment data incorrectly.

6.3 Driver Assistance Literature Review

ADAS has four different tiers of operation. The first is a no action tier when the vehicle is on course and no foreign objects are encroaching on the vehicle. The second tier is driver warning system that is initiated when undesirable behavior is detected. The third tier is vehicle controlling a few minor aspects of normal navigation such as speed control and lane keeping assist. The fourth tier is an emergency override when the driver has not responded to alerts. An example of this is frontal collision avoidance. There are many different modules of ADAS for object avoidance, however, the only commercially available modules that are dedicated to keeping the vehicle on the road are the lane departure warning (LDW) and the lane keeping assist (LKA) modules. These two modules are effectively identical except that LKA has the ability to steer the vehicle back into the lane, whereas LDW is a warning system using optical or audible signals to inform the driver.

In current LDW systems the driver is alerted based on certain thresholds defined by the vehicle. In order for these thresholds to be calculated, information from the road must be extracted and modeled. This is the main focus of research in the field of LDW as it is the most complex part of the system. If the road model is incorrect then the warning system will have no chance of working properly.

There are many LDW systems that have been researched. Most use forward facing cameras to gather information about the lane edge markings. The obvious implementation of a camera is to optically see that part of the vehicle is over the lane edge in much the same manner that humans do. The other use of optics is to obtain data regarding the lane edges. This lane data is used to develop a mathematical representation lane boundaries. Near fields can be modeled as

linear functions as the road doesn't change very quickly over a very short distance, therefore linear functions are an accurate representation for those short segments. More complex functions are used to model the extended road lane edges where linear functions no longer are accurate enough. One implementation of this combines a linear near field prediction and a parabolic curve for far field estimation [44, 45]. These lane approximations are used to both locate the vehicle within the lane and also determine what dynamic control is expected to navigate the upcoming road. Another, more simplistic, use of lane edge data extraction is to calculate the relative orientation of the left and right lane edge relative to the camera perspective to approximate the vehicle's location within the lane and estimate a time to lane change [45-47].

LDW systems can also be based on a measured vehicle and road position. In addition to using sensors to view the road edges the current position of the vehicle is compared to a high level map to determine whether or not the vehicle is off the road. Using GPS to detect lane departures using a combination of accurate mapping data and a vehicle GPS unit is a commonly researched technique. [48-52]. There are many small differences in the techniques used to increase GPS accuracy and localize the vehicle within the lane to determine whether the vehicle has left or is close to leaving the road.

6.4 Driver Warning System Development

The goal of this ADAS is to alert the driver or take over control of the vehicle if the vehicle is conducting unsafe behavior. The development of this system based off the road data will be transmitted to the vehicle for the next section of road, including local x and y data, road curvature, road heading angle and additional layers. A few assumptions where made in this development and simulation. The first is that the road data that the vehicle receives is one hundred percent accurate compared to the actual road geometry. Another assumption is that there are no foreign hazards in the path of the vehicle, i.e. pedestrians, other vehicles, etc. We also

assume that the road surface is ideal and there are no bumps or other disturbances that could set the vehicle off course. It is assumed that the vehicle knows its position relative to the desired path with absolute certainty as our initial focus is to develop thresholds based on the outcomes rather than the reliability of position. In the development of thresholds related to vehicle friction capacity, the aerodynamic effects on down force or lift are neglected and it is assumed that the normal force of the vehicle is only related to vehicle weight and ground slope, however the need of aerodynamically based speed limit is discussed.

6.4.1 Requirements

At the basis of this ADAS system are thresholds that determine whether or not the occupant is in danger. This is based on the information that the vehicle has regarding its current environment. With a regulated and verified road geometry data set transmitted to the vehicle, the same process can be accomplished more accurately. Therefore, we will discuss the thresholds that we determined provided effective means of keeping the vehicle on course.

There are some criteria that we want our system to be capable of accomplishing. The ADAS system needs to be able to monitor when the vehicle is about to depart its current lane and notify the driver of the error or take its own corrective action. It also needs to have additional parameters that will help identify vehicle instabilities and other issues that will cause the vehicle to lose control or exit its lane. In this way the system can have a predictive nature to its alert system rather than just alerting when something has already gone wrong.

6.4.2 Vehicle instabilities

6.4.2.1 Excessive Speed

One threshold that is important to determine is if the vehicle is carrying too much speed into a particular curve. Speed is an important factor with respect to the turn radius of a vehicle.

As curvature of the road increases, as long as the vehicle maintains the same speed, the lateral acceleration of the vehicle increases with the following relationship for a level surface:

$$a_{lat} = V^2\kappa \tag{6.1a}$$

$$a_{lat} = lateral\ accelration\ \left(\frac{ft}{s^2}\right) \tag{6.1b}$$

$$V = Speed\ \left(\frac{ft}{s}\right) \tag{6.1c}$$

$$\kappa = Road\ curvature \tag{6.1d}$$

Lateral acceleration creates a lateral force in the vehicle. This force is resisted by the lateral friction force between the tires and the road surface. However, tires have a maximum friction limit controlling tire-road traction. Once the limit is surpassed the vehicle will slide out of control of the driver. The National Traffic Safety Administration (NHTSA) has a formula that prescribes a maximum vehicle speed threshold for a given road configuration.

$$V_c = \sqrt{gR\frac{e+f}{1-ef}} \tag{6.2a}$$

$$V_C = maximum\ safe\ speed \tag{6.2b}$$

$$g = gravitational\ acceleration\ constant\ \left(\frac{ft}{s^2}\right) \tag{6.2c}$$

$$R = minimum\ radius\ of\ a\ curve\ (ft) \tag{6.2d}$$

$$e = superelevation\ of\ a\ curve \tag{6.2e}$$

$$f = prescribed\ side\ friction\ factor \tag{6.2f}$$

This formula compensates for the fact that vehicle roll angle increases on elevated curves, allowing for additional speed capacity. Additionally, it accounts for the side friction factor that is prescribed by AASHTO which applies a factor of safety to the maximum amount of lateral friction force needed. However, this is a safe speed that works under all road conditions. If this were to be set as the speed threshold for ADAS engagement it would be constantly violated by drivers and be more of a nuisance than it would be helpful.

Therefore, a threshold needs to be developed that allows for elevated speeds so that the driver is only notified when they will not be able to safely transverse an upcoming curve. A passive system may permit the driver to travel in excess of the speed limit but a warning may be issued if the excessive speed limit leads to increased risk of departing the road in advance of an upcoming curve. In contrast, an autonomous system may prohibit speeds in excess of the annotated speed limit on a roadway. A future manifestation of this system would include the option for locally reducing a speed limit due to events such as lower traction (rain, ice, sleet, reports of slickness, or hydroplaning); construction zones; or safer transportation around partially closed lanes from EMS use.

Elevated speeds can result in a lift force imposed on the vehicle from the pressure differential between the top and bottom surfaces of the vehicle. This negatively affects the control capacity of the vehicle as normal force transmitted through tires is reduced. Vehicle with higher center of gravities and high ground clearance are particularly susceptible to this as it allows more air flow under the vehicle. As a result, an autonomous system may utilize formulaic approaches to determining safe travel speeds based on lane and road curvatures. Likewise, if unsafe environmental conditions indicate that the safe travel speed is below a minimum value for the given roadway and vehicle combination (example: high crosswinds on a freeway with curves for large truck vehicles), alternative routes could be recommended to avoid the potential for

dynamic tip-over events. It will be up to the manufacturers to determine what this top speed limit should be as it is dependent on the specific vehicle model.

Another threshold should be developed based on the verified data regarding the road ahead by predicting the vehicles ability to negotiate the upcoming roadway. A vehicle's ability to successfully negotiate a specified curve is dependent on the vehicle's speed and steering system characteristics. In cornering there are three types of vehicle behavior: neutral steer, understeer and oversteer. For a constant-radius turn if vehicle speed is increased the steering input must remain the same, increase, or decrease for the three vehicle behaviors respectively. Most vehicles on the roadway follow an understeer behavior, thus it will be the configuration of interest. When cornering at high speeds there is a point at which no matter how much more the driver steers, the vehicle cannot turn anymore. This is a result of the friction between the tires to ground reaching full capacity. Therefore, there is no more available friction force available to counteract the increased lateral acceleration. This is a point that is not desired to be reached as the vehicle will not be able to be stably controlled.

In designing road for specific speeds according to AASHTO guidelines they use a .15 friction coefficient as a safe metric for allowable side friction [31]. This metric is equivalent to the amount allowable lateral g-force experienced by the vehicle. It is assumed that for an average vehicle (no significant tire wear) and for an average road surface that the maximum total available friction coefficient is around one. The typical friction experienced by the vehicle need to be kept much lower so that it has left over capacity should it need to make any dynamic maneuvers. A very small portion of this limit goes to the longitudinal movement of the vehicle as the vehicle accelerates forward due to wheel slip that occurs at constant speeds as well as when accelerating. A change of allowance in lateral acceleration could be a metric in which its alteration would increase the maximum travel speed.

However, lateral wheel slip occurs before friction capacity is reached. Therefore, a more accurate measure by which to predict the vehicle's ability to traverse a curve is to use the understeer modified Ackerman equation [29].

$$\delta = 57.3L\kappa + Ka_y \tag{6.3a}$$

$$\delta = Front\ wheel\ steer\ angle\ (\text{deg}) \tag{6.3b}$$

$$L = Wheelbase\ (ft) \tag{6.3c}$$

$$\kappa = Turn\ Curvature\ \left(\frac{1}{ft}\right) \tag{6.3d}$$

$$K = Understeer\ gradient\ \left(\frac{deg}{g}\right) \tag{6.3e}$$

$$a_y = Lateral\ acceleration\ (g) \tag{6.3f}$$

This accounts for lateral wheel slip in the vehicle. This formula can be used to predict whether the vehicle has the physical capacity to traverse the upcoming curve given its current speed and steering limits. The physical steering limits should then be compared to the estimated wheel angle, as it should not strain the physical limits. For low speeds, the percentage of allowable angular wheel steer is greater than is allowed for higher speeds as the minimum safer turn radius increases. An inversely proportional relationship between speed and percent difference between steering angle based on the prescribed road speed can be applied so that the higher the speed, the less leeway the driver will have before being alerted to slow down.

6.4.2.2 Roll Over

In addition to the maximum friction limit, roll over parameters of vehicles affects the vehicle speed limit heading into a curve. Vehicle roll instability occurs when the normal force

corresponding to one side of the vehicle transmitted to the tires is equal to zero. Vehicle stabilization forces are shown schematically in figure 6.1. This will result in the vehicle rolling over onto the side of the vehicle or even further. This also results in loss of vehicle control as one side the vehicle no longer has any potential for friction development.

Roll stability is primarily dependent on the lateral acceleration of the vehicle as it impacts vehicle weight distribution as the vehicle corners. A vehicle propensity for roll over is dependent on the track width and center of gravity height as they effect the magnitude of the moment that force resulting from lateral acceleration. The wider the track width and the lower the center of gravity the more lateral acceleration is needed to overturn the vehicle. A critical speed is defined for roll over instability at which there is no normal force on one side of the vehicle.

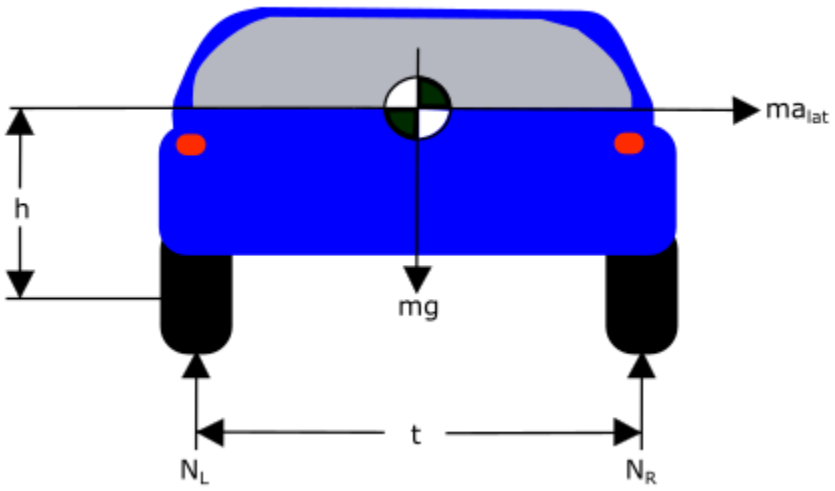

Figure 6.1 Track Width Vehicle Model

- h- vehicle c.g. height
- g- gravity
- m- vehicle mass
- a_{lat}- lateral acceleration
- t- track width
- N_L- normal force left
- N_R- normal force right
- V_crit – critical roll speed

$$N_R = N_L = \frac{mg}{2} \qquad \text{*for a stationary vehicle} \tag{6.4a}$$

$$ma_{lat}h = \frac{mg}{2} + mg\frac{t}{2} \tag{6.4b}$$

$$a_{lat} = \frac{V_{crit}^2}{R} V = Speed\ \left(\frac{ft}{s}\right) \tag{6.4c}$$

$$V_{crit} = \sqrt{\frac{Rgt}{h}} \tag{6.4d}$$

This formulation does not account for road slope, which would allow for a higher critical velocity for roll over. However, by excluding road slope this metric is given a factor of safety. Therefore, as a recommended vehicle limit, the vehicle critical road speed for a given curve should be used to set a speed limit warning when approaching a curve.

6.4.3 Departure Thresholds

6.4.3.1 Orientation Error

A measure that is helpful in predicting potential road departures is orientation error. Orientation error is difference between the ideal heading angle of the roadway and the current heading angle of the vehicle as described in figure 6.2.

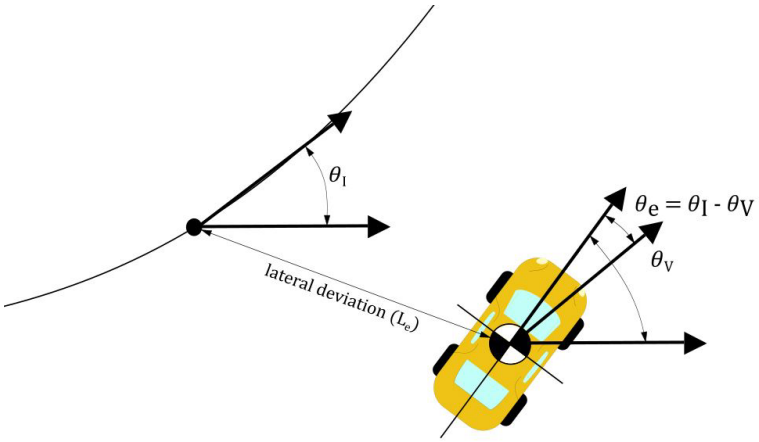

Figure 6.2 Heading Error and Lateral Deviation

$\theta_e = \theta_I - \theta_V$

$\theta_e = heading\ angle\ error$

$\theta_I = ideal\ heading\ angle$

$\theta_V = vehicle\ heading\ angle$

Using the realistic AASHTO roadway data, heading angle error was multiplied by the vehicle speed and to determine lateral deviation rate. For small values of angles, heading angle error is proportional to departure rate. Departure rates, on a straight road segment, as a function of heading angle error with respect to the tangent road heading is shown for various speeds in figure 6.3. Given a lane width of 12 ft., when driving at low speeds it takes a significant heading error to leave the roadway. At highway speeds, drivers have less room for error as a small error will result in departing the road in less than second.

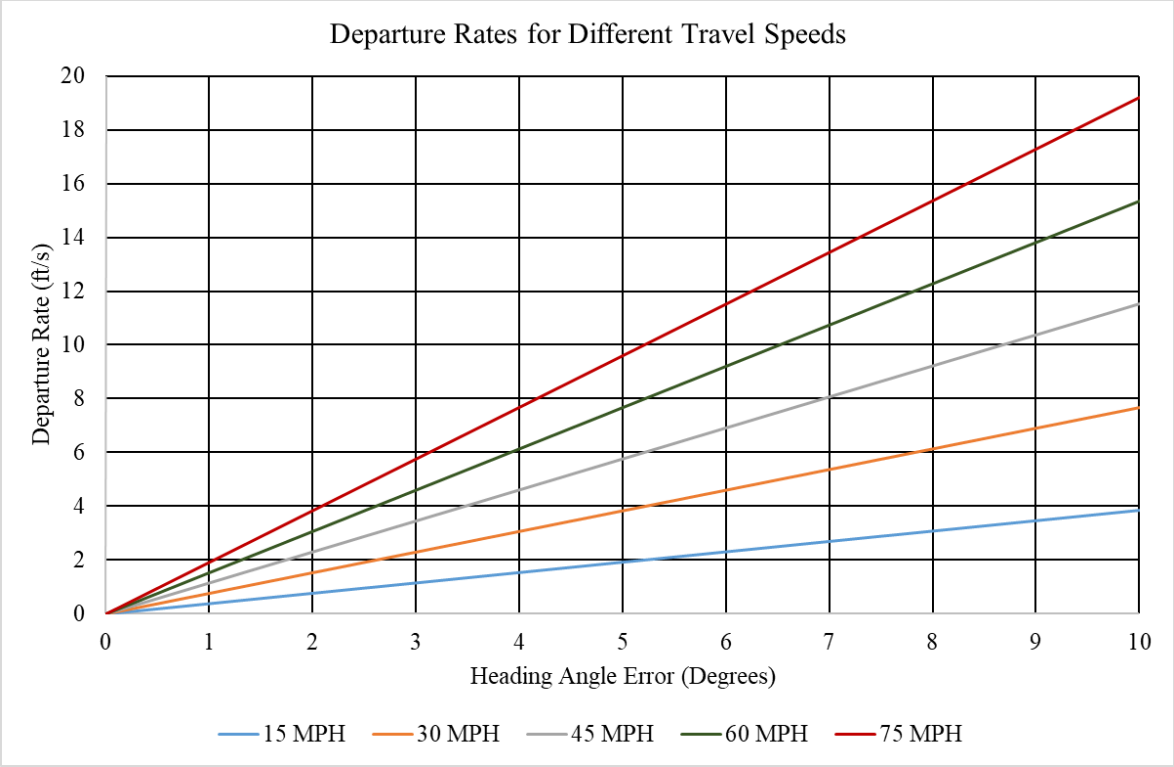

Figure 6.3 Departure Rate According to Heading Angle Error

Figure 6.4 shows how the heading angle error manifests itself visually in comparison to the tangent road heading. It is much easier as a driver and for a computer to predict a road departure at low speeds since the angle is much more significant. As a driver decreases the magnitude of heading error necessary to depart the road within a couple of seconds, the resolution required by a computer in order to detect a potential departure also magnifies. Human driving behavior is imperfect, as people do not perfectly mimic the centerline trajectory of the road. Instead, the typical driving behavior is to gradually oscillate around the centerline. Therefore, some heading angle error is expected and they could easily incur an error of a few degrees at a given moment, complicating the prediction for the computer. Additionally, a singular departure threshold may not always be applicable. Depending on the current position of the vehicle on the road and the width of the road the driver may need to be warned sooner.

Heading error from the road tangent path could be used as a signifier for predicting if the vehicle is trending out of its lane, however, it cannot be based on instantaneous error alone.

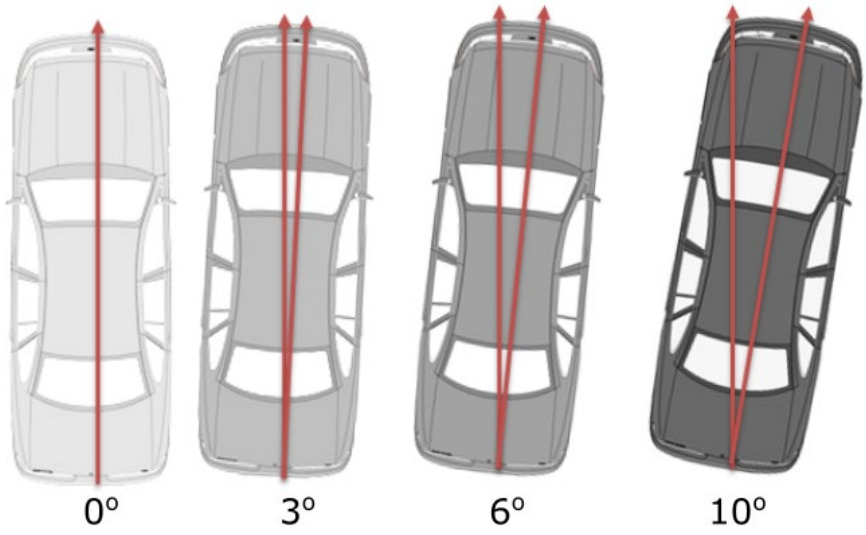

Figure 6.4 Visual Depiction of Heading Angle Error

6.4.3.2 Rate of Change in Heading Angle

When using heading angle error as a road departure characteristic the rate at which it is changing is a useful metric to separate normal driving characteristics from a departure. Typical driving behavior can be characterized by a slow oscillation around the lane centerline of the vehicle. Therefore, under normal driving behaviors the rate of change in heading angle will also change as well but not trend in any particular direction. The departure heading angle error rate will be a relatively constant value in the case of a straight road, and a constantly increasing measurement in the case of a curved roadway. So, the rate of change in heading angle can be used to filter out false positives. A time lapse of constant direction, positive or negative, for a predetermined time threshold can be set to alert the driver before leaving the roadway, however this is complicated by current vehicle position and road geometry. It could, however, be used in a

secondary check to the current heading angle error and providing a time to lane change through curve fitting the recorded rate for the times steps since the last sign change. Once the function is approximated it would again warn the driver if a departure is predicted in less than one second.

6.4.3.3 Change in acceleration

Another measurement that can also help predict a roadway departure is the change in lateral vehicle acceleration over time. The reason that this is useful is that road curve transitions are traditionally built off of a desired change in later acceleration as it is a measure of ride comfort and safety. The equation as presented in AASHTO for calculating the necessary transition length is as follows:

$$L = \frac{3.15V^3}{RC} \tag{6.5a}$$

$$L = minimum\ length\ of\ transition\ (ft) \tag{6.5b}$$

$$V = vehicle\ speed\ (mph) \tag{6.5c}$$

$$R = curve\ radius\ (ft) \tag{6.5d}$$

$$C = rate\ of\ increase\ of\ lateral\ acceleration\ \left(\frac{ft}{s^3}\right) \tag{6.5e}$$

In designing spiral transitions, the maximum increase in lateral acceleration usually ranges between 1 and $3\frac{ft}{s^3}$. It is another metric that can be used to determine whether the vehicle is following the desired path according to design standards or not. When components of the change in lateral acceleration is integrated over time it is possible to predict the future heading angle of the vehicle and calculate the error to the desired orientation error.

$$\frac{da_{lat}}{dt} = V^2 \frac{d\kappa}{dt} = V\left(V \frac{d\kappa}{dt}\right) \tag{6.6a}$$

$$V \frac{d\kappa}{dt} = \frac{\Delta rad}{s^2} \tag{6.6b}$$

$$\frac{\Delta rad}{s^2} \Delta s \Delta s = \theta_V \tag{6.6c}$$

As previously discussed, heading angle error is proportional to departure rate. By using lateral acceleration, predictions on what the future rate of road departure could be based on current dynamics.

6.4.3.4 Lateral Deviation

Vehicle deviation from the desired trajectory is an important characteristic as it is the ultimate determination of vehicle safety with regards to staying on target. In the scenario of slow and gradual departure, it is the only subsystem that will detect the issue because the short-term vehicle behavior is stable.

In order to determine the lateral deviation from the path the vehicle computer uses the XY data that it received from the infrastructure network in the beginning of the route and compares it to its current XY position in the local framework. After calculating the relative error between the desired road path and vehicle position, the component of the error measurement that is normal to the road path is used to determine the lateral error.

$$x_e = (x_r - x_v) \tag{6.7a}$$

$$y_e = (y_r - y_v) \tag{6.7b}$$

$$\begin{pmatrix} e_{tangent} \\ e_{lateral} \end{pmatrix} = \begin{pmatrix} \cos\theta_I & -\sin\theta_I \\ \sin\theta_I & \cos\theta_I \end{pmatrix} \begin{pmatrix} x_e \\ y_e \end{pmatrix} \tag{6.7c}$$

$$(x_r, y_r) - road\ position \tag{6.7d}$$

$$(x_v, y_r) - vehcile\ position \tag{6.7e}$$

$$(x_e, y_e) - position\ error \tag{6.7f}$$

$$(e_{tangent}, e_{lateral}) - tangent\ error\ and\ lateral\ error \tag{6.7g}$$

Current lateral deviation is a vital part of the system as other departure metrics are dependent on the current lateral deviation to predict the time road departure. It also the used as the last line of defense, so to speak, meaning that if the vehicle behaves in such a way no other thresholds are triggered, such as the vehicle is on or over the lane boundary, the lateral deviation threshold will trigger an alert. This threshold should be set to trigger when the vehicle has deviated enough to be on the lane boundary.

6.5 Safe Stop Scenarios

The purpose of most of the developed thresholds, excessive speed, orientation error, and change in lateral acceleration is to determine whether or not the driver should be warned of unsafe behavior and to take corrective action. No control of the vehicle is taken over by the computer system as there is only potential for a safety hazard.

In the case of excessive lateral deviation, road departure has already occurred. If at this point no drive input has been detected the vehicle computer must take over control to bring the vehicle to a safe stop. A safe stop is a maneuver in which the vehicle is brought to a controlled stop while being steered to the side of the roadway so that it does not interfere with traffic. The point at which this takes place is a complex question as it is dependent on the particular vehicle as well as the road configuration. These factors need to be accounted for in the development of a safe stop protocol.

Different road configurations affect when the safe stop occurs. In the case of a large road shoulder, with no nearby roadside hazards, the vehicle could be allowed to venture over the road edge and onto the shoulder before the computer takes control. However, the opposite scenario occurs on narrow mountain roads that have no shoulder and the vehicle has a smaller error window before a safe stop can be invoked.

In additional to the roadside configuration the lane configuration also plays an important role. One of the outcomes of the safe stop is bringing the vehicle to the side of the road, however if the vehicle is traveling on a road with multiple lanes, the vehicle cannot automatically deviate to the side of the road to stop if it is in an interior lane. In this instance the vehicle would slow down to a creep pace instead of a full stop until it determines that it is safe to change lanes and make its way to the side of the road. This process would require the use of either external proximity sensors or vehicle to vehicle (V2V) communication to determine if there are any vehicles in the relative proximity before making any maneuvers.

6.6 Emergency Stop Evaluation

Simulations were conducted to investigate road departure characteristics. A common scenario that was investigated is for an inattentive driver on a curve. This simulation assumes that the driver is not responsive to departure alerts. This scenario is explored to determine at what point an ADAS needs to take over control, and what kind of control input is necessary to prevent the vehicle from running off of the road.

The first simulation does not apply ADAS control until the outside tires of the vehicle are on the shoulder of the road, a lateral deviation of 6 ft on a 12 ft wide road. Once the vehicle reaches this point, full braking is applied with no steering input. It is assumed that the maximum deceleration rate is 1 G. The road that was used in this simulation was an AASHTO regulated curve designed for travel speeds of 60 mph. The road is a transition designed for the highest

allowable change in lateral acceleration as the road transitions from a straight lane to a constant radius curve.

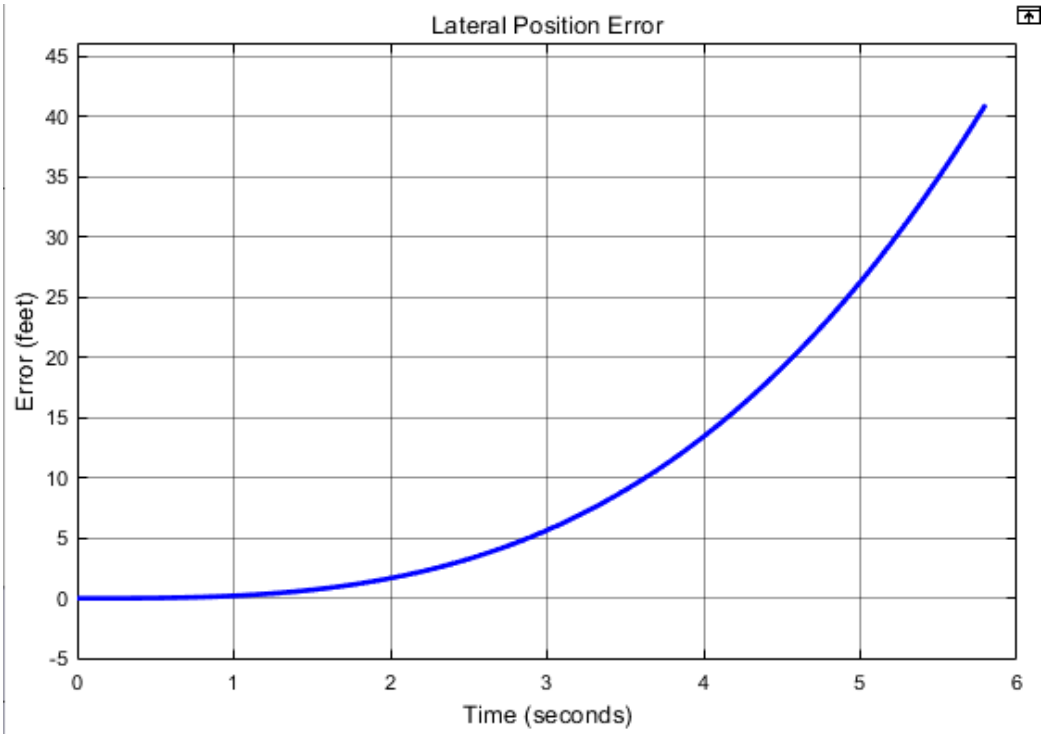

Figure 6.5 Lateral Position over Time

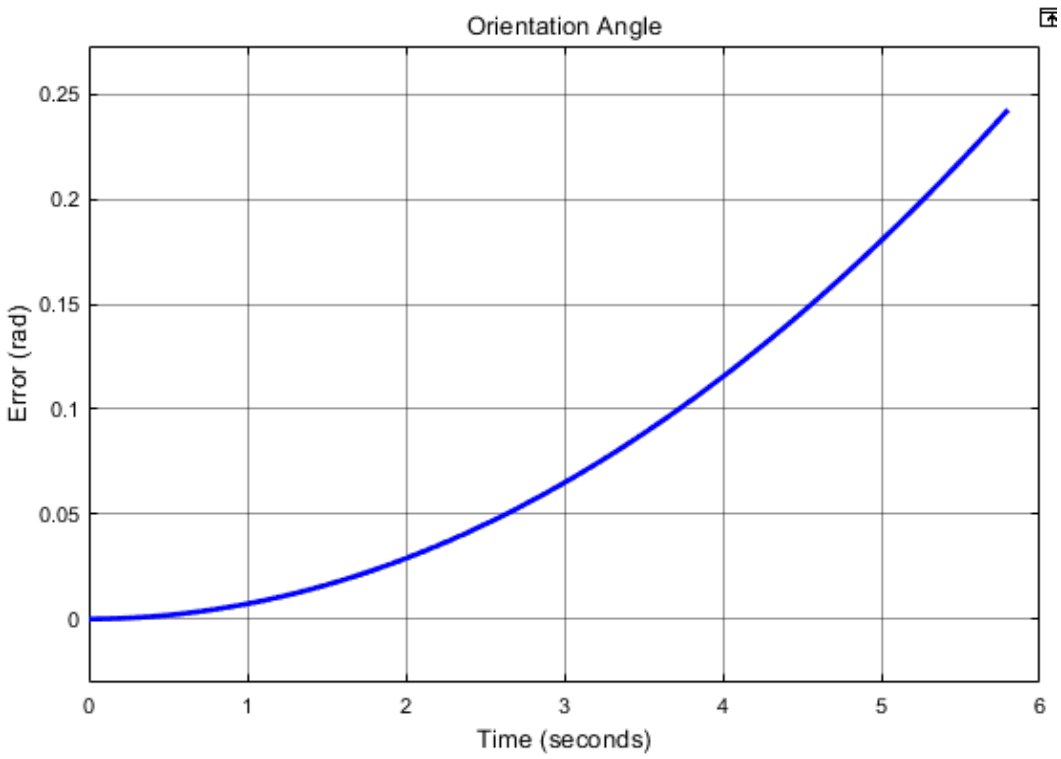

Figure 6.6 Orientation Angle over Time

The vehicle starts in the middle of the lane and gradually drifts to the side of the road if no steering correction is made as it travels. The vehicle position reaches the outer road boundary in approximately three seconds as seen in figure 6.5. It is interesting to note from figure 6.6 that the orientation angle error reaches a maximum value of 0.07 radians (4 degrees) at that point. Even though the orientation is small, a road departure occurs over time because orientation error persists. When the vehicle reaches the road edge it slows at a rate of 1 G. The emergency stop protocol is not evoked until this point to allow for as much lateral deviation as possible before braking. Even though the vehicle is slowing down, the rate of deceleration is still increasing because the curve radius is increasing and therefore the road heading is changing faster as the vehicle travels forward. When the vehicle comes to a complete stop the lateral error is at its overall peak of 41 ft, at which point the vehicle has far exceeded the lane boundary

When braking from 60 mph the vehicle takes 2.8 seconds to stop. Based on the departure results in figure 6.6, in order for the vehicle to be stopped without any part leaving the roadway the brakes would need to be applied before even an inch of deviation occurs. Therefore a steering input also needs to be applied in an emergency stop protocol to stop the vehicle on or near the road. This will be discussed in further sections as the vehicle steering control is developed.

6.6.1 Threshold Summary

Discussed in this section were various metrics by which drivers can be alerted or the vehicle computer takes over control to remain on the roadway. The next step in this series to drive real vehicles with necessary sensors to capture the data needed to determine which predicted thresholds would be the most effective in being the support structure of an ADAS.

6.7 Vehicle control development and literature review

An effective AV system has two goals. The primary goal is to operate the vehicle so that the occupants are kept safe. The second goal is do so in such a manner so that the occupants can experience a comfortable ride.

6.7.1 Control methods

6.7.1.1 PID Control

One of the most common control methods used in industry is the Proportional Integral Derivative (PID) controller. PID controllers are a feedback controller, meaning that the output variable(s) of the system are fed back to the control which prompts a new control command into the system. The control structure is based on the error from the desired system output. The goal of a PID controller is to minimize that error. It accomplished this by taking the error, the derivative of error, and the integration of error with respect to time along with three individual gain constants and combining them to a system input as shown below:

$$i(t) = K_p E(t) + K_d \frac{dE(t)}{dt} + K_i \int E(t)dt \tag{6.8a}$$

$$i(t) = system\ input \tag{6.8b}$$

$$E(t) = system\ error \tag{6.8c}$$

$$K_p = proportionial\ constant \tag{6.8d}$$

$$K_i = integral\ constant \tag{6.8e}$$

$$K_d = derivative\ constant \tag{6.8f}$$

PID controllers are modified to fit the specific system it controls by tuning the gain constants to achieve the desired output. The main performance factors that are considered when tuning a PID controller are rise time, overshoot, settling time, and steady-state error. Rise time is the time required to reach the desired output value, when error is zero. Overshoot occurs when the system output reaches the desired value, but the system doesn't stop and overshoots the target. This occurs due to system inertia and the system doesn't stop at the desired value. Settling time is the time it takes for the system output to settle and remain with a certain percentage of the desired output, usually 10%. Finally, steady state error is the remaining error between the current output value and the desired value after the control process is finished.

The proportional constant, K_p, is adjusted to minimize rise time, the larger the K_p, the faster the output will reach the desired value. However, a higher value will result in a magnified overshoot value. The primary objective of the integral constant, K_i, is to reduce steady state error. If a small error remains in the system, it is integrated over time and that small error will grow, allowing the controller to compensate for it. The derivative constant, K_d, is to reduce overshooting and settling time [53]. It affects the control output based on the derivative of error

over time so as the error approaches zero it reduces the amount of correction allowing for a smoother control.

PID is advantageous as it is simplistic, meaning that it takes less computing time and power to achieve accurate results. This is important as intelligent vehicles need to be able to make decisions quickly. However, this simplicity negatively affects the controller's ability to control complex and nonlinear systems.

6.7.1.2 MPC Control

Another common control method used in intelligent vehicles is Model Predictive Control (MPC). MPC again works to achieve a desired outcome by minimizing the error between the desired behavior of the system and the actual outcome. This is done by first inputting the future trajectory path. The prediction horizon is a metric that dictates how far into the future the control extracts information in order to make decisions. The controller uses this future data to create a schedule of control steps for every time step to achieve the end result. This allows the controls step to be optimized to work together to efficiently control the system. The controller then applies the first control step to the system before re-optimizing the control schedule, taking into account the next additional times step [54]. An example of this is shown in figure 6.7. MPC is particularly useful for vehicle control due to its ability to handle specified constraints. In the control parameters hard and soft constraints can be prescribed so that the model will not violate key aspects of travel like road deviation, speed limit, and other vehicle limits.

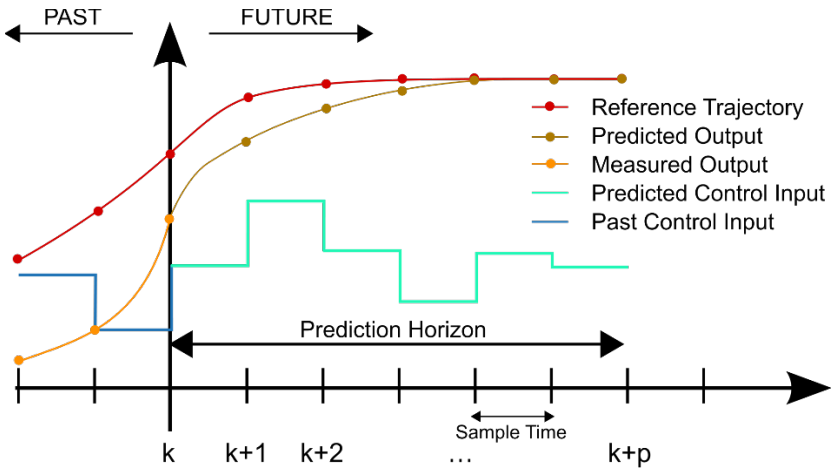

Figure 6.7 Example of MPC Prediction and Control [55]

The major drawback of MPC control is that it is more computationally expensive as it re-optimizes the predicted control for every time step. This can be remedied by reducing the length of the prediction horizon; however, this negates the benefits and advantages of this control method aspect.

6.7.2 Correction Methods

6.7.2.1 Stanley method

One particular method to guide an autonomous vehicle is known as the Stanley method. This method applies a correction to regain the desired path based on heading error and cross track error, governed by the following equation:

$$\delta(t) = \theta_e(t) + \tan^{-1}\left(\frac{ke_{fa}(t)}{v_x(t)}\right) \tag{6.9a}$$

$$\theta_e = heading\ error \tag{6.9b}$$

$$e_{fa} = cross\ track\ error \tag{6.9c}$$

$$v_x = forward\ velocity \tag{6.9d}$$

$$k = correction\ factor \tag{6.9e}$$

The correction factor k is then altered by either increasing for a higher degree of correction or by decreasing for a smaller correction effect [56].

6.7.2.2 Pure Pursuit

Pure pursuit is a very common navigation method used in robotics. This method works by setting a path of data points. The current position of the vehicle is then used to calculate the radius of curvature of a path from the vehicle position and is used to estimate the wheel angle to achieve the target point. This is geometrically demonstrated in figure 6.8 while desired steering angle is then calculated as follows [56]:

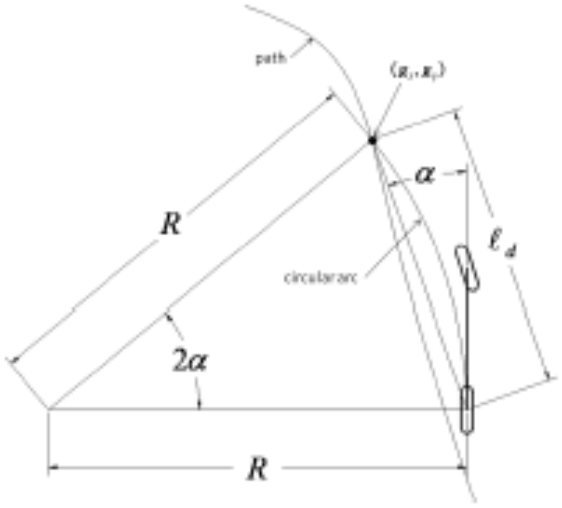

Figure 6.8 Pure Pursuit Controller Geometry [56]

$$\delta(t) = \tan^{-1}\left(\frac{2Lsin(\alpha)}{\kappa v_x(t)}\right) \tag{6.10}$$

Pure pursuit is tuned by modifying look ahead distance. The look ahead distance determines how far ahead into the prescribed path the controller looks. This metric is very sensitive to the road geometry and needs to be tuned to the specific nature the roadway. If the look ahead distance is too short, the vehicle will tend to oscillate excessively due to small curve radii. If the look ahead distance is too long, the vehicle will not accurately track with the current vehicle path [57].

6.7.3 Road Model

The road data used in the ADAS development is based on the model of a standard road design based off American Association of State Highway and Transportation Officials (ASHTO) guidelines to ensure a realistic road geometry. The particular road that was used is characterized by a gradual transition from a straight path to a constant radius curve followed by a transition back to a straight road. The particular road was designed based on travel at a 60 mph with a super-elevation of 12 and a side friction factor of 0.12 resulting in a minimum curve radius of 1,000 ft [31]. These values were chosen to simulate the smallest radius possible for the given speed so that the system would be evaluated at the limits that the vehicle would experience for a given speed. The simulated curve is shown in figure 6.9.

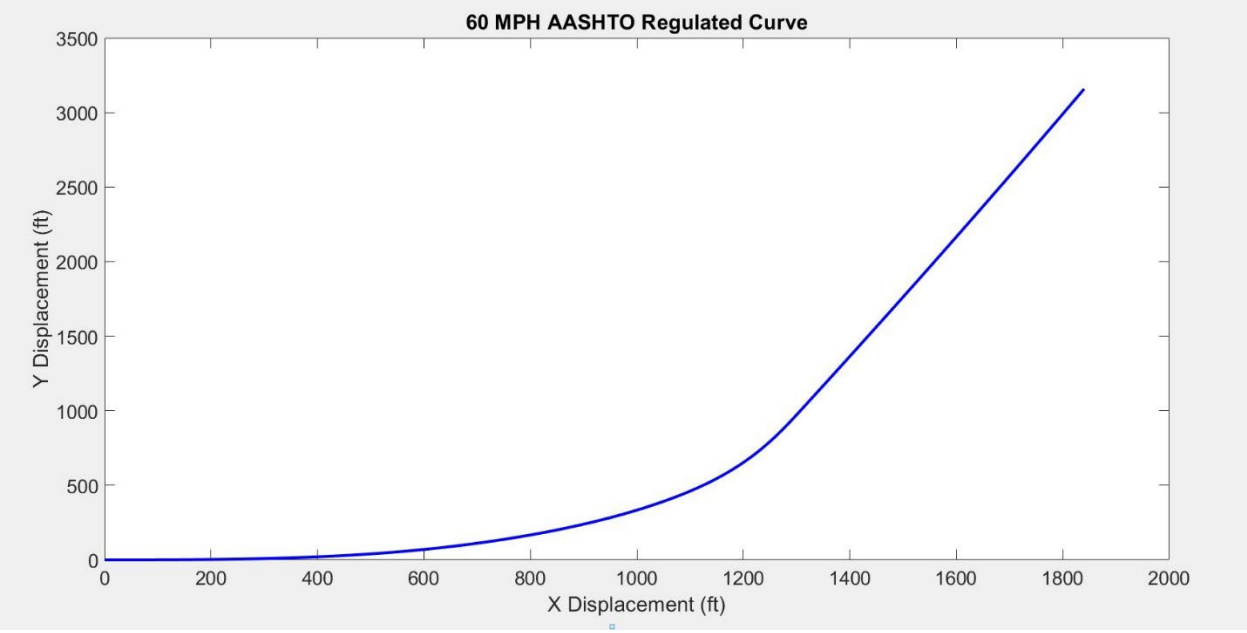

Figure 6.9 Road Data XY Data

The local XY data of the road was used to calculate the curvature as seen in figure 6.10 and road tangent heading angle, figure 6.11. These metrics will be broadcast to the vehicle in the full system. This is one of the metrics that will be sent to the vehicle in the full system implementation. In initial simulations, curvature was used to help control the vehicle by using a simple approximation to determine the steering behavior. Road heading will be used to serve as a reference to determine the heading error of the vehicle to further control the vehicle behavior.

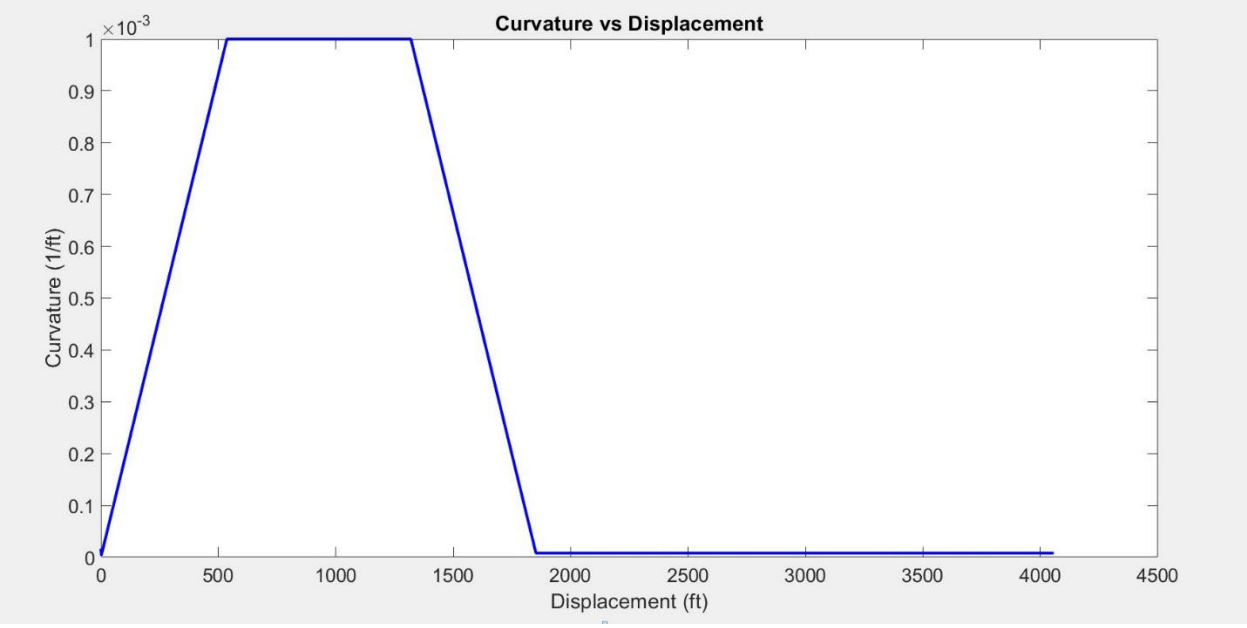

Figure 6.10 Road Curvature Data

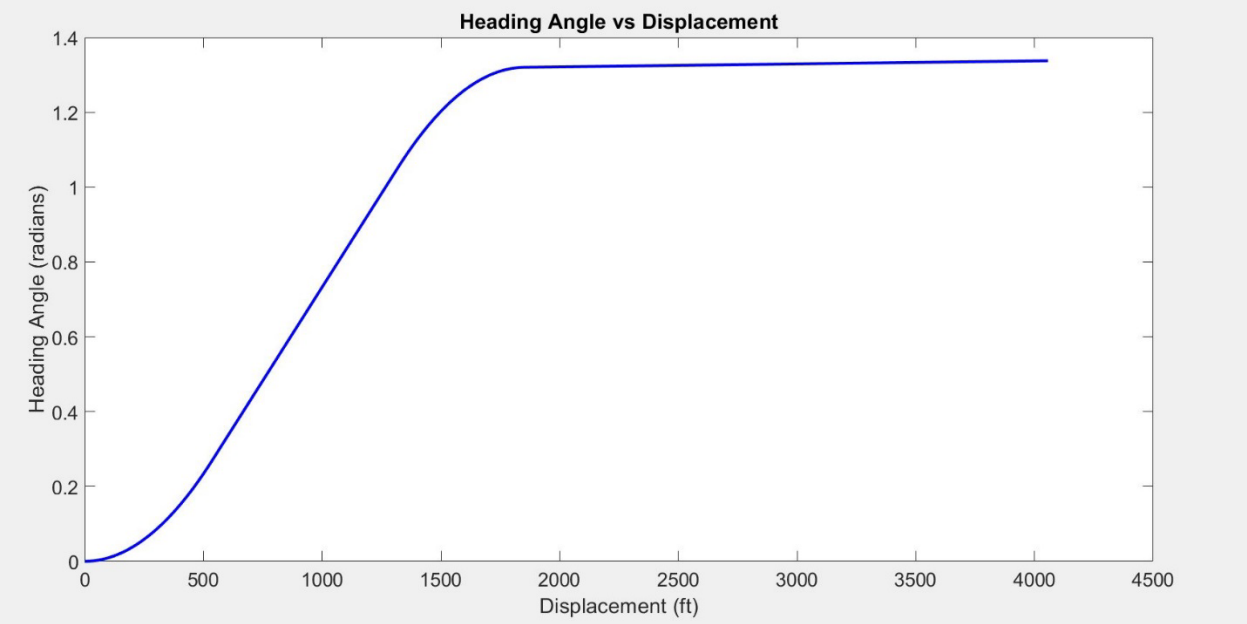

Figure 6.11 Heading Angle Data

6.7.4 Vehicle Model

The model used for developing a vehicle control system is the bicycle vehicle model. The bicycle model is created by combining the front and rear axles of a vehicle together as seen in figure 6.12.

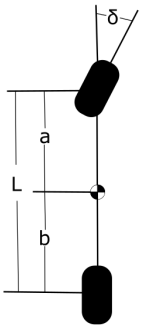

Figure 6.12 Bicycle Model

The vehicle can be simplified in this manner because under stable conditions a vehicle's cornering ability is dependent on wheel angle and wheelbase. At elevated travel speeds this relationship is distorted due to lateral slip experienced between the wheels and the roadway and is related to lateral acceleration. This modification is dependent on specific vehicle geometry characterized by the understeer gradient [29]. These factors are combined to define a desired wheel angle in the understeer modified Ackerman equation:

$$\delta = 57.3L\kappa + Ka_y \tag{6.11a}$$

$$\delta = Front\ wheel\ steer\ angle\ (\text{deg}) \tag{6.11b}$$

$$L = Wheelbase\ (ft) \tag{6.11c}$$

$$\kappa = Turn\ Curvature\ \left(\frac{1}{ft}\right) \tag{6.11d}$$

$$K = Understeer\ gradient\ \left(\frac{deg}{g}\right) \tag{6.11e}$$

$$a_y = Lateral\ acceleration\ (g) \tag{6.11f}$$

The specific vehicle geometry that was used in the model was based off the C-Class Hatchback 2012 template found in CarSim. This specific model has a wheelbase of 9.55 ft. The vehicle was simulated in CarSim and was found to have an average understeer gradient of 1.46 deg/g for the given road geometry previously described.

6.7.5 Model Development

The control method used in the system was a PID controller. This method was chosen as it allows for a gradual ramp up and ramp down control, similar to how a human driver operates a vehicle. It also is effective in eliminating steady state error which plays a big factor when controlling over miles of road allowing for error to gradually build up if not corrected. Road data previously developed was used as the inputs into the system. The overall system utilizes three independent PID controllers that are each based on the error from the wheel angle, future wheel angle and lateral deviation error respectively as seen in figure 6.13.

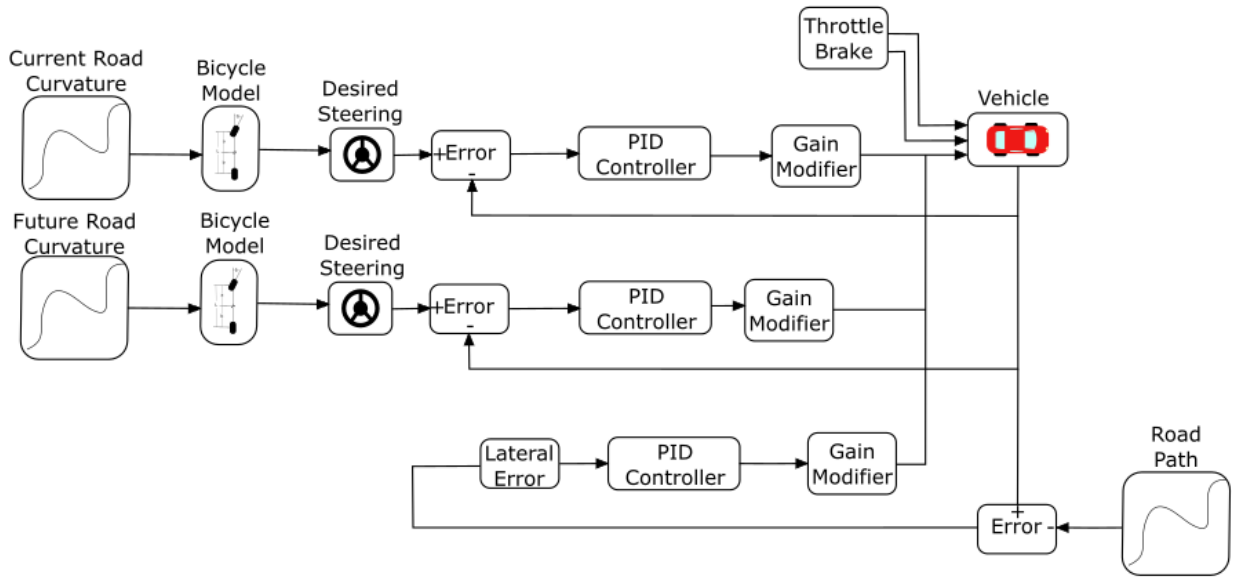

Figure 6.13 Vehicle Control Schematic

The first PID controller was based on the desired wheel angle needed to achieve a turn curvature equivalent to the current curvature of the road based on the modified Ackerman steer equation. In this system, error is calculated between the current vehicle wheel angle and the current desired wheel angle. This error is input to the PID controller and an updated wheel angle is input into the vehicle system. The PID controller parameters, which can be seen in table 6.1, were tuned in order to have a fast rise time as this is critical for staying on the road as delay in control is reverberated in road departure. This control was mainly dependent on the proportional gain parameter.

The second PID controller was based on the future desired wheel angle needed to achieve a turn curvature of the road, again based on the modified Ackerman steer equation. The control of this parameter is identical to the previous PID controller and the same gain parameters are used as the same overall goal is identical as shown in table 6.1. This additional controller helps the vehicle compensate for the fact that the road is constantly changing at a high rate of speed.

Therefore, by the time the previous controller has gone through the process of inputting the new desired wheel angle, adjusting the steering angle to the optimal angle the position with the corresponding steering adjustment is already long gone and it is already time for a new input. Adding in a future angle parameter allows the system to begin to progressively control the vehicle to start to steer in advance but not so much as to cause a large amount of lateral error.

The third input of control into the system is the minimization of lateral error to the path. This is a highly necessary part of staying on the desired path. Even if the heading angle and turn curvature has reached zero error the vehicle can still have residual error spatially related to the desired path. Minimizing lateral error keeps the vehicle on the road and prevents error from accumulating as the vehicle travels along the road.

The road reference used in the calculation of lateral error is the nearest road coordinate relative to the current position of the vehicle. The XY coordinates have been rotated according to the heading angle of the roadway, the lateral error becomes collinear with the curvature vector of the roadway and therefore is normal to the desired path. The magnitude of control associated with this error is far less than used in the previous PID controllers. The constants found to be the most effective and stable for the lateral error controller can be seen in table 6.1.

The output of each of the controllers are individually weighted to achieve the desired output. In this simulation it was assumed that the bicycle model was an accurate representation of the necessary steering input in order to stay in on the road. Therefore, the current steering angle serves as the primary mode of control in the system and mainly dictates the steering wheel angle into the vehicle system.

The next tier of control impact is the future desired wheel angle. This is given second priority based on the previous reasoning for the current wheel angle. However, the weight associated with this controller is far less in magnitude because if too much magnitude is used the

vehicle would potentially rely too much on the on the future road and leave the current roadway as a result.

The final controller based on the lateral error has the smallest impact on the system based on its weight relative to the others. The theory behind this control scheme is that given a current road curvature, the necessary wheel angle to remain on the road can give a reasonable starting point to controlling the vehicle. Lateral deviation is then used to supplement this by essentially nudging the vehicle in the right direction by adding additional control into the system. A summary of the control parameters can be seen in table 6.1.

Table 6.1 Controller Parameters

	Constant	Value	Gain Modifier
Wheel Angle Controller	P	60	1
	I	1	
	D	3	
Future Wheel Angle Controller	P	60	0.015
	I	1	
	D	3	
Lateral Error Controller	P	10	0.01
	I	0	
	D	10	

The system was designed using three independent PID controllers to serve as a check and balance system. As mentioned before, it is assumed that the bicycle model provides a reasonable estimation of the necessary wheel angle. When the future wheel angle and lateral error controller supplement this control, the steering wheel angle error is increased as a result. Therefore, the primary controller will try to adjust its own control further to fight against the other controllers. Theoretically this will result in minor and gradual correction in the system because the additional controllers serve to bound the control of the primary.

6.8 Results of Simulation

6.8.1 Standard Control Scenario

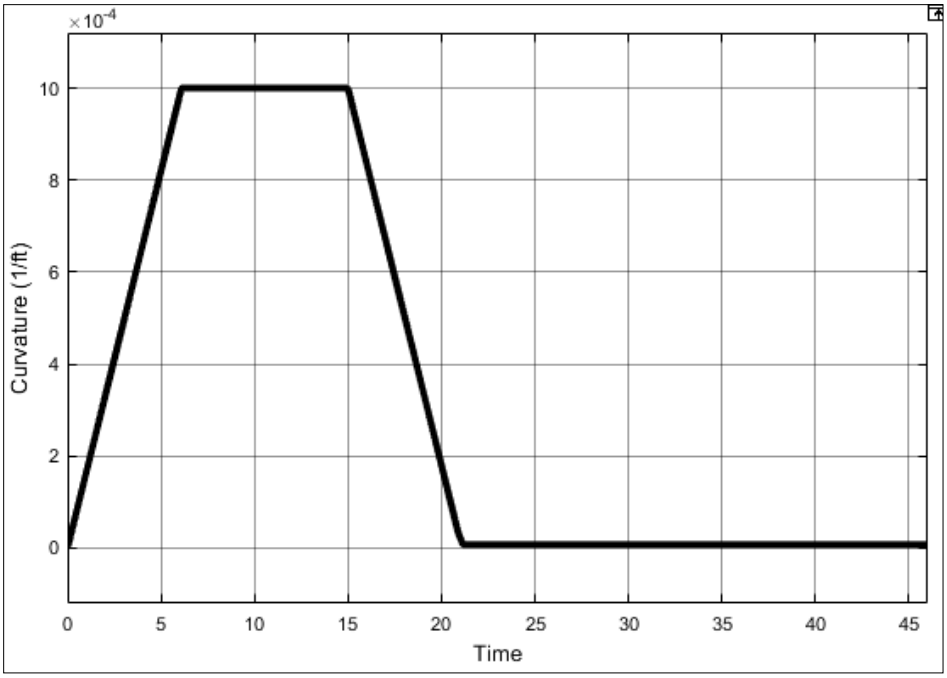

Figure 6.14 Road Curvature vs. Time

We can see in this plot that the road starts as straight with the curvature beginning at approximately zero. The road curvature then linearly increases until a road curvature of $1.0\ X\ 10^{-3}\ \frac{1}{ft}$. Curvature is then held constant for a period of time before starting to decrease until it is equal to approximately zero and then held constant for a period of time once again. This curvature plot is representative of an AASHTO regulated road for a vehicle operating at 60 mph. This indicates that the vehicle is following the proper curvature trend of the roadway without any significant error or oscillatory nature indicating that the controller is capable of controlling the vehicle with enough speed and accuracy.

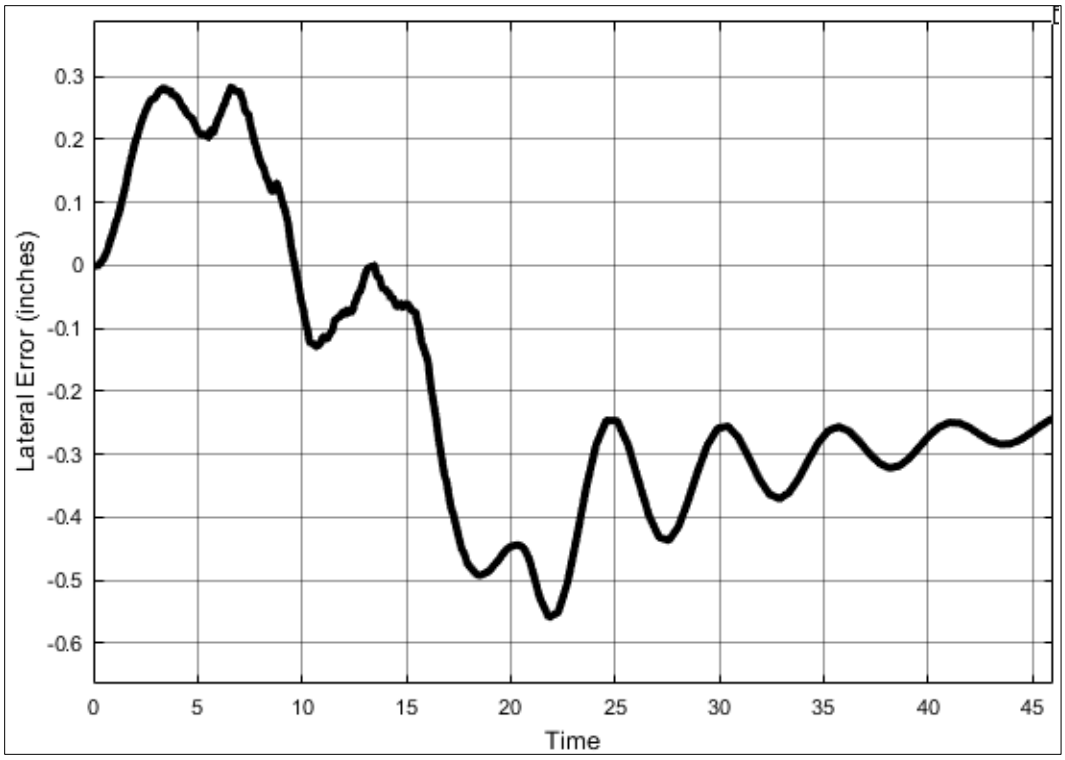

Figure 6.15 Lateral Deviation from Lane Center

Figure 6.15 shows the lateral deviation from the desired path which corresponds with the lane center of the given road. This is the first metric that is used to determine if the controller was successful. It can be seen in this plot that the vehicle maximum lateral deviation from the lane center was 0.56 inches. This is well within the desired lateral error of 6 inches. Additionally, the behavior of the curve itself indicates that the lateral movement of the vehicle is stable and there are no excessive spikes or oscillations indicating the loss of control.

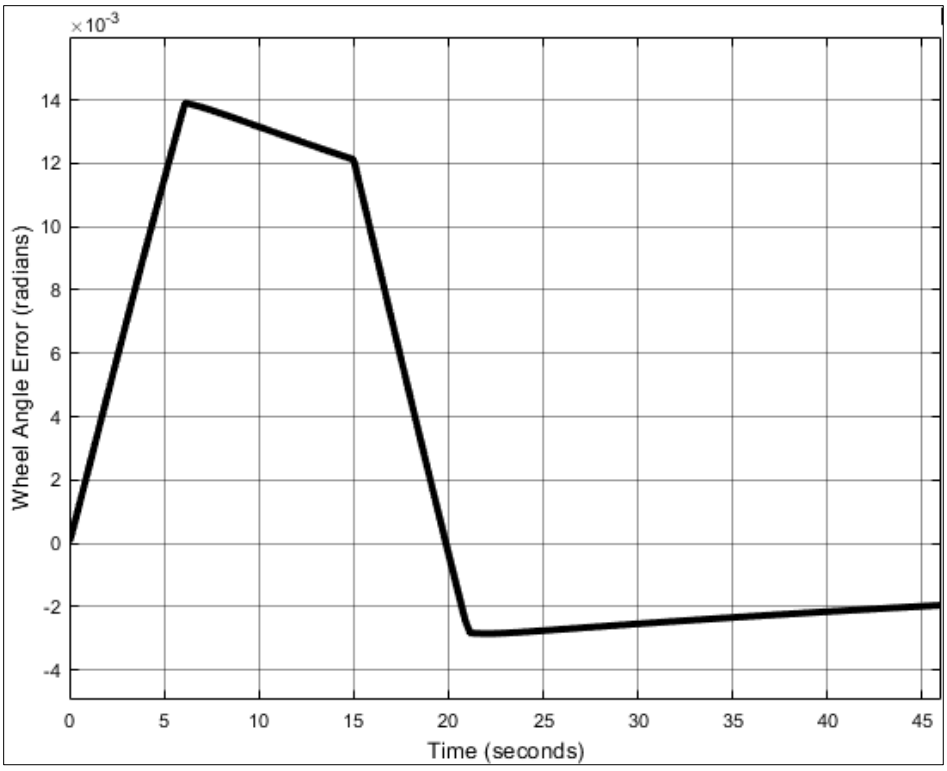

Figure 6.16 Wheel Angle Error from Current Desired Wheel Angle

The actual vehicle wheel angle was then compared to the ideal wheel angle. It should be noted that the ideal wheel angle is not equivalent to the desired wheel angle that is output from the PID controller as the controller creates a delay because a physical system cannot achieve a given value instantaneously.

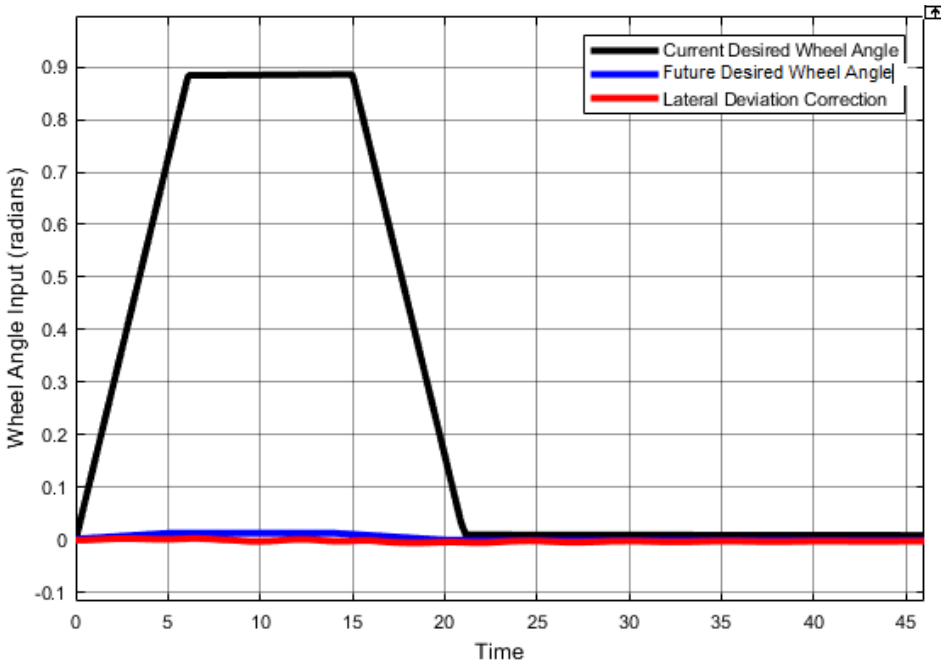

Figure 6.17 Wheel Angle Inputs

The desired wheel is the primary metric for keeping the vehicle on the target path, as mentioned before, however, additional correction is still needed. The two supplementary controllers are used to supplement the control and increase the tracking accuracy of the vehicle. In figure 6.17 the current wheel angle is the most dominant control input and the other inputs work to nudge the steering input in the correct direction to compensate for actual vehicle behavior.

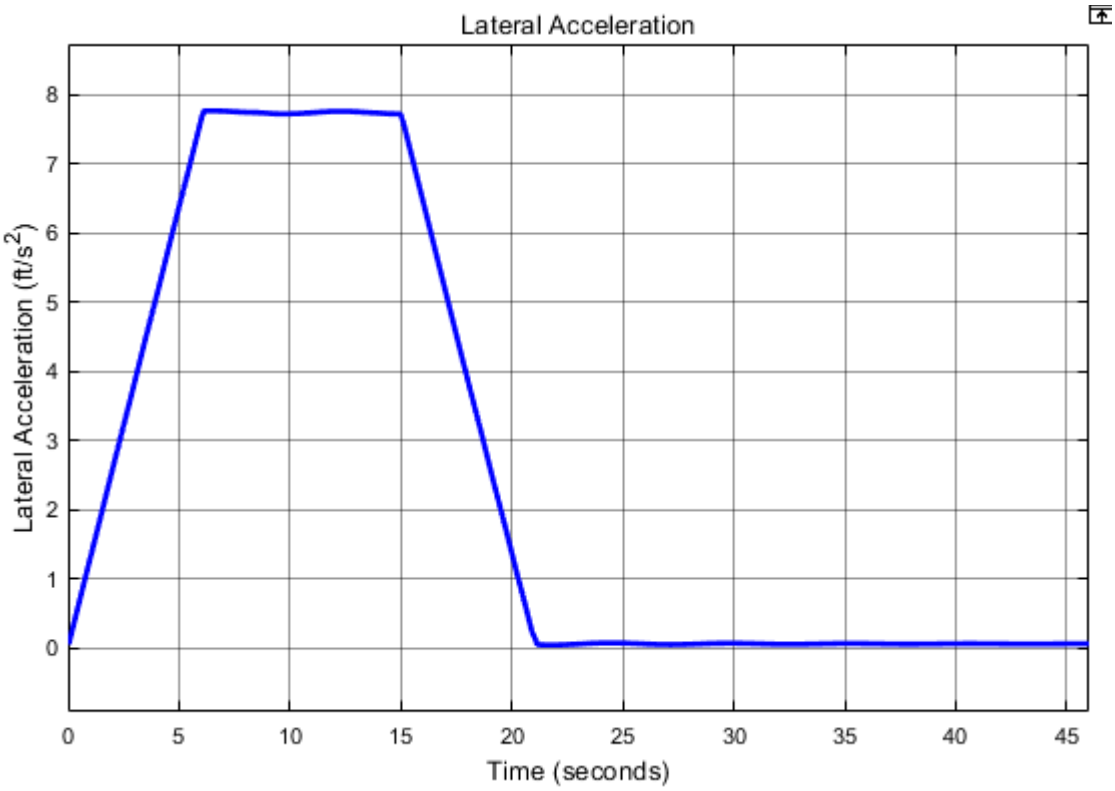

Figure 6.18 Lateral Acceleration over Time

Lateral acceleration impacts vehicle stability and ride comfort. If lateral acceleration oscillates, the vehicle occupants will experience significant discomfort and will not adopt the autonomous system. Lateral acceleration oscillation can also instigate roll over instability as quick, significant directional changes in lateral acceleration cause the vehicle C.G. inertia to lag the friction development of the tires. Therefore, it is important to minimize lateral acceleration oscillation. It can be seen in figure 6.18 that lateral acceleration throughout the curve follows the expected acceleration according to $a_{lat} = \frac{V^2}{R}$ without significant abnormalities indicating a smooth stable ride.

6.8.2 Emergency Stop Control

As demonstrated in Section 6.6, in order for an emergency stop to be executed by an ADAS that is not constantly in control of the vehicle, a steering correction is necessary to stop the vehicle on the road. This control method is based on the vehicle control structure disclosed in section 6.9.3. This structure was implemented to stop the vehicle once it reached a lateral deviation of 6 ft from the desired path. The magnitude of error significantly affects the stability of the PID controller. The control needs to be adjusted to compensate for this higher error so it doesn't cause the vehicle to become unstable trying to correct itself. The tuned constants for the three controllers are shown in table 6.2. When compared to the constant values in table 6.1 the proportional gain for the desired wheel angle was reduced to slow the speed of the steering correction. The derivative constant was increased slightly to improve correction behavior.

Table 6.2 Emergency Stop Control Parameters

	Constant	Value	Gain Modifier
Wheel Angle Controller	P	10	1
	I	0	
	D	3	
Future Wheel Angle Controller	P	60	0.015
	I	1	
	D	3	
Lateral Error Controller	P	10	0.01
	I	0	
	D	15	

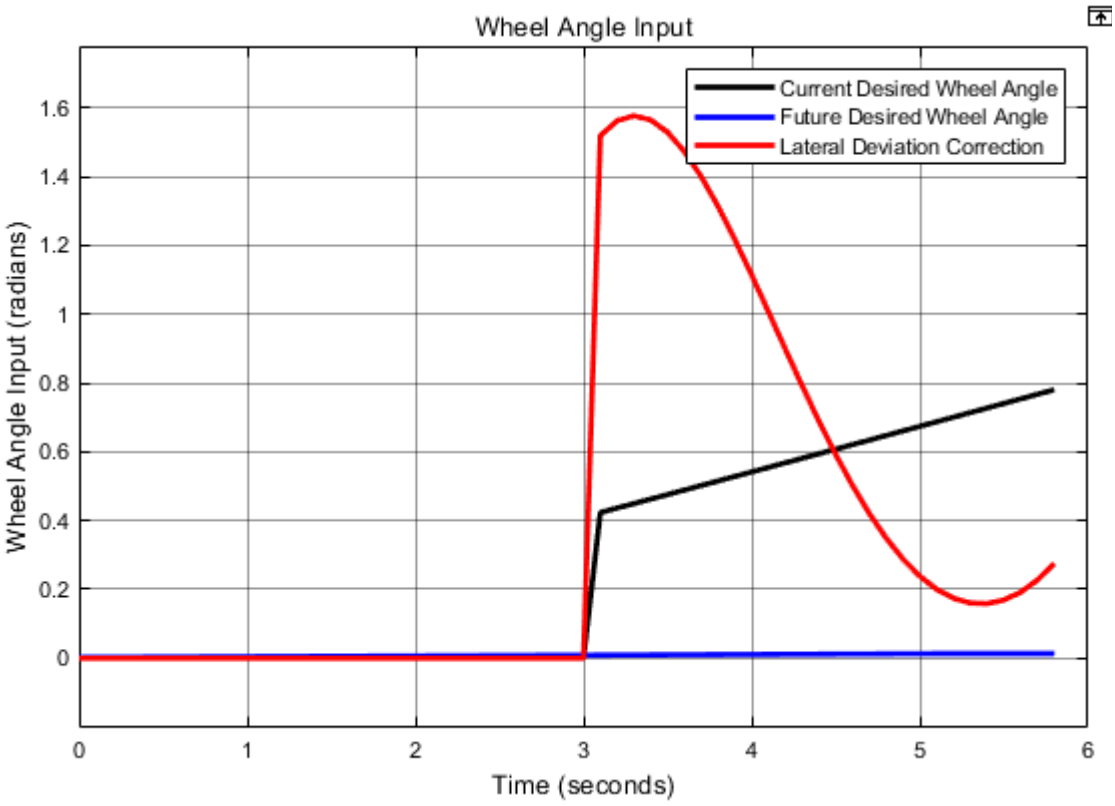

Figure 6.19 Wheel Angle Inputs for Emergency Stop

Shown in figure 6.19 are vehicle steering inputs. Unlike the previous model, the control is now dominated by the lateral error correction. This makes sense as the difference in steering angle for a transition curve will not be very significant. This is the desired behavior for this scenario because the vehicle controller needs to make correcting the lateral deviation the top priority in order to remain on the road.

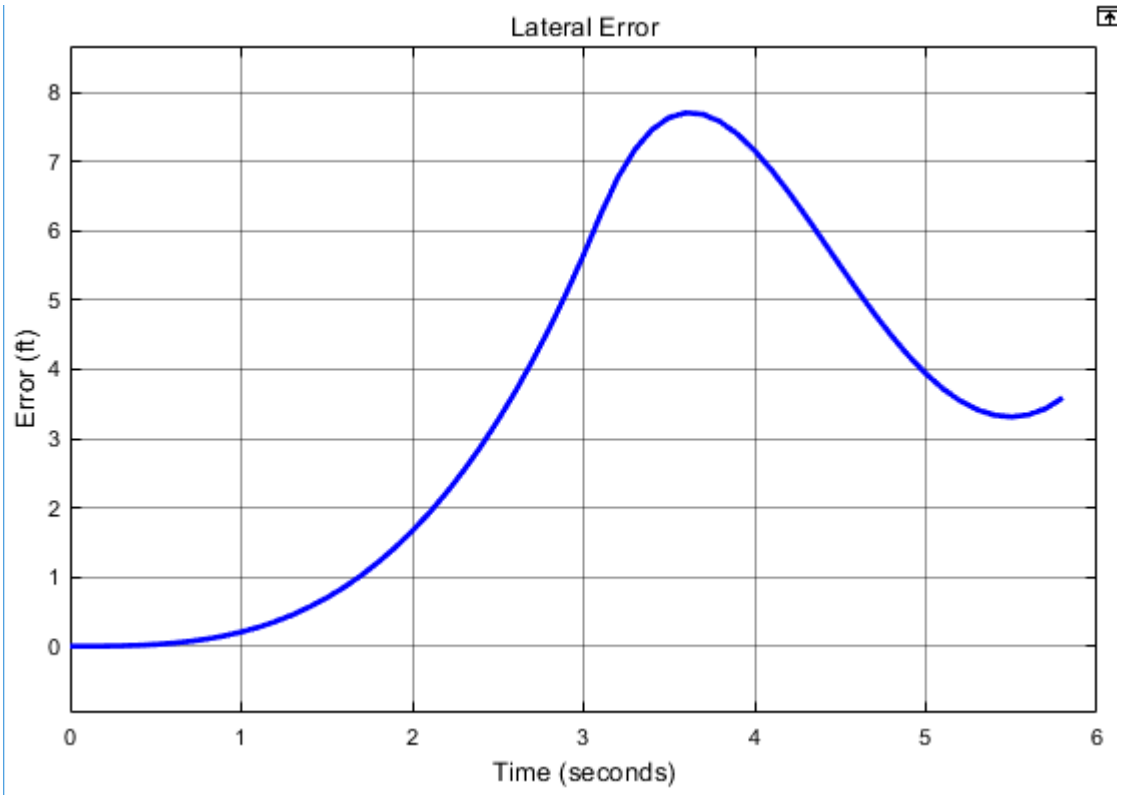

Figure 6.20 Lateral Error during Emergency Stop

When the steering control is applied to the emergency stop the minimizing is clearly tremendously improved comparing figure 6.5 and figure 6.20. The vehicle still proceeds past the outer road edge by 1.7 ft which is not allowable in certain environments when the vehicle cannot cross over the road edge. Increasing the aggressiveness of the controller to turn more quickly towards the roadway creates over shooting issues and therefore is not ideal. To properly prevent the road boundary additional metrics were discussed in previous sections of this report. These metrics should be tested with a real driver to determine the impact they have on deterring road departures before a vehicle intervention is necessary.

Chapter 7 Summary and Future Work

7.1 Summary

7.1.1 Path Generation

This section is focused on a technique for generating a discrete, curvature-dependent path from an offline database information such as GPS or geographical scans. The technique was developed from geometric formulations implemented from Google Earth data. The technique is further developed with AASHTO guidelines to increase accuracy and comply with dynamic tire limits. Results showed that this method provides a reasonable guidance heading angle for vehicles.

7.1.2 Vehicle Control

In order to determine the feasibility of the proposed road data technique a control system was developed in two phases. The first phase was the use of the road data to develop potential thresholds for an ADAS whose operation is to warn the driver of unsafe driving behavior and safety stop the vehicle in the case of an imminent road departure. The metrics developed for departure warning were based on the following:

- Excessive Speed
- Roll Over Stability
- Heading Angle Error
- Lateral Acceleration
- Lateral Deviation

The impact of each of these thresholds were individually discussed for how they can contribute to a driver alert system and recommendations for threshold values were disclosed. Further evaluation, with live vehicle testing, is needed to refine the recommended thresholds

after accounting for real driver and vehicle handling behavior. The secondary part to the ADAS system was the discussion of necessities to govern an emergency vehicle stop in various scenarios. The active vehicle control in these scenarios was also developed in conjunction with an autonomous control system.

In addition to developing departure warning characteristics a vehicle guidance structure was also developed to study the use of the proposed road data model for autonomous vehicle travel. Using the road data developed in Chapter 5, a multiple PID control structure was simulated for controlling a vehicle throughout an AASHTO regulated curve.

The disclosed vehicle control structure was able to adequately control the vehicle model throughout the entire curve stably with a maximum deviation from the target path of less than one inch, well within the desired limits for vehicle travel to stay in lane. This control model can help provide a base point for live vehicle testing.

References

1. United States Department of Transportation, Roadway Departure Safety, Available:<https://safety.fhwa.dot.gov/roadway_dept/>July 23, 2018.

2. *Fatal Accident Reporting System (FARS) Encyclopedia*, National Highway Transportation Safety Administration (NHTSA), 2016. http://www-fars.nhtsa.dot.gov/Main/index.aspx

3. *Roadway and environment*: *Fatality Facts*, Insurance Institute for Highway Safety, Highway Loss Data Institute. https://www.iihs.org/topics/fatality-statistics/detail/collisions-with-fixed-objects-and-animals

4. Stolle, C.S., Lechtenberg, K.A., Faller, R.K., and Yim, T., "Initial Developments Supporting a Roadside Tree Removal Safety Campaign", Presentation to the 1st International Roadside Safety Conference, San Francisco, California, June 2017. Accepted for Publication in the Journal of the International Conference of Roadside Safety.

5. Andrews, S., *Vehicle-to-Vehicle (V2V) and Vehicle-to-Infrastructure (V2I) Communications and Cooperative Drivering,* Handbook of Intelligent Vehicles, Eskandarian (ed), Springer-Verlag, London, 2012. DOI 10.1007/978-0-85729-085-4_46

6. *V2V/V2I Communications for Improved Road Safety and Efficiency*, Jurgen, R.K., (ed), Society of Automotive Engineers, Warrendale, PA, 2012. ISBN 978-0-7680-7725-4

7. Devilly, O., and O'Mahony, M., *Assessing the Benefits of Installing V2I Communications on an Urban Orbital Motorway in a Medium Sized European City*, Journal of the Transportation Research Board, Washington, D.C., January 2018

8. *SAE International, Surface Vehicle Recommended Practice J3016,* June 2018.

9. Sweigard, M.E., Jacome, R.O., and Stolle, C.S., *MATC Year One Report, Final Report to Mid-America Transportation Center*, MwRSF Research Report No. MwRSF-40042-01, University of Nebraska-Lincoln, Lincoln, Nebraska, October 2018.

10. GPS.GOV, GPS Accuracy, Available: <https://www.gps.gov/systems/gps/performance/accuracy/> 09/18/2019

11. Computerworld, Black Hat Europe: It's easy and costs only $60 to hack self-driving car sensors, Available: <https://www.computerworld.com/article/3005436/black-hat-europe-it-s-easy-and-costs-only-60-to-hack-self-driving-car-sensors.html> 09/18/2019

12. S. Temel, M.C. Vuran, M.M.R. Lunar, Z. Zhao, A. Salam, R.K. Faller, and C.S. Stolle. "Vehicle-to-Barrier Communication during Real-World Crash Tests". Computer Communications. August 2018. DOI: 10.1016/j.comcom.2018.05.009

13. M. Werling, J. Ziegler, K. Soren, and S. Thrun. *Optimal Trajectory Generation for Dynamic Street Scenarios in a Frenet Frame*, 2010

14. A. Kelly, B. Nagy, *Reactive Nonholonomic Trajectory Generation via Parametric Optimal Control*, 2003

15. Y. Sun, Z. Zhan, Y. Fang, L. Zheng, L. Wang, G. Guo, *A Dynamic Local Trajectory Planning and Tracking Method for UGV Based on Optimal Algorithm*, 2019

16. A. Takahashi, T. Hongo, Y. Ninomiya, G. Sugimoto, *Local Path Planning and Motion Control for AGV in Positioning*, 1989

17. A. Piazzi, C. Guarino lo Bianco, *Quintic G2-Splines for Trajectory Planning of Autonomous Vehicles*, 2000

18. D. Wilde, *Computing Clothoid-Arc Segments for Trajectory Generation*, 2009

19. H. Delingette, M. Hebert, K. Ikeuchi, *Trajectory Generation with Curvature Constraint based on Energy Minimization*, 1991

20. L. J. van Vliet, P. W. Verbeek, *Curvature and Bending Energy in Digitized 2D and 3D Images*, 1993

21. P. Guillaume, J. Schoukens, R. Pintelon, *Sensitivity of Roots to Errors in the Coefficient of Polynomials Obtained by Frequency –Domain Estimation Methods*, 1989

22. K. E. Atkinson, *An Introduction to Numerical Analysis*, 1989

23. Weisstein, Eric W. "Spherical Coordinates." From *MathWorld*--A Wolfram Web Resource. http://mathworld.wolfram.com/SphericalCoordinates.html

24. Google Earth, Location for MwRSF Design Headquarters, 40.821726° N -96.689624° W, viewed January 2020.

25. Polyline, API from Google Developers for Android. From *Google Developers.* https://developers.google.com/android/reference/com/google/android/gms/maps/model/Polyline, accessed January 2020.

26. O'Reilly, O.M. Engineering Dynamics: A Primer. Springer Science & Business Media, 2010.

27. Pressley, A.N. Elementary Differential Geometry. 2nd ed. Springer Undergraduate Mathematics Series. London: Springer-Verlag, 2010. https://doi.org/10.1007/978-1-84882-891-9.

28. Pacejka, H.B. Tyre and Vehicle Dynamics. Butterworth-Heinemann, 2006.

29. Gillespie, T.D. "Fundamentals of Vehicle Dynamics," SAE Int. ISBN 1-56091-199-9, 1992.

30. do Carmo, M.P. Differential Geometry of Curves and Surfaces. 1st ed. Englewood Cliffs, N.J: Prentice-Hall, 1976.

31. A Policy on Geometric Design of Highways and Streets, (The Green Book) 6th ed. American Association of State Highway and Transportation Officials, 2011.

32. Are Mjaavatten (2019). Curvature of a 2D or 3D curve (https://www.mathworks.com/matlabcentral/fileexchange/69452-curvature-of-a-2d-or-3d-curve), MATLAB Central File Exchange. Retrieved May 24, 2019.

33. M. Duhn, G. Parikh, J. Hourdos, *I-94 Connected Vehicles Testbed Operations and Maintenance*, 2019

34. Druta, A. S. Alden*, Implementation and Evaluation of a Buried Cable Animal Detection System and Deer Warning Sign*, 2019

35. SAE International, *J3016-Taxonomy and Definitions for Terms Related to Driving Automation Systems for On-Road Motor Vehicles*, 2018

36. William J. Hughes Technical Center, *Global Positioning System (GPS) Standard Positioning Service (SPS) Performance Analysis Report*, 2017

37. Heinrich, S., "Planning Universal On-Road Driving Strategies for Automated Vehicles," AutoUni – Schriftenreihe. Springer, 2018. https://doi.org/10.1007/978-3-658-21954-3.

38. *Model S Owner's Manual*, Tesla Inc., May 2019

39. *Accord 2018 Owner's Manual*, Honda Motor Company, December 2017..

40. *Toyota 2018 Camry From July 2017 Prod. Owner's Manual (OM06122U)*, Toyota Motor Corporation, July 2017.

41. *2018 Altima Sedan Owners' Manual and Maintenance Information,* Nissan Motor Company, November 2017.

42. *2018 Malibu Owner's Manual*, General Motors, Plymouth, MI, 2017.

43. 2019 Fusion Owner's Manual, Ford Motor Company, 2018.

44. Jung, C. R., and Kelber, C. R., *A Lane Departure Warning System on A Linear- Parabolic Lane Model*, 2004 IEEE Intelligent Vehicles Symposium, Parma, Italy, June 2004, pages 891-895.

45. Jung, C. R., and Kelber, C. R., *A Lane Departure Warning System Using Lateral Offset with Uncalibrated Camera*, October 2005.

46. Somasundaram, G., Kavitha, and Ramachandran, K. I., Lane Change Detection and Tracking for a Safe-Lane Approach in Real Time Vision Based Navigation Systems, First Interantional Conference On Computer Science, Engineering And Applications 2011, Chennai, India, 2011, pages 345-361.

47. Kwon, W., and Lee, S., *Performance Evaluation of Decision Making Strategies for an Embedded Lane Departure Warning System*, Journal of Robotic Systems 19(10), 2002, pages 499-509.

48. Clanton, J. M., Bevly, D. M., and Hodel, A. S., *A Low-Cost Solution for an Integrated Multisensor Lane Departure Warning System*, IEEE Transaction on Intelligent Transpiration Systems, Vol. 10, No. 1, March 2009, pages 47-59.

49. Faizan, M., Hussain, S., and Hayee, M. I., *Design and Development of In-Vehicle Lane Departure Warning System using Standard Global Positioning System Receiver*, Journal of the Transportation Research Board, 2019.

50. Wang, J., Schroedl, S., Mezger, K., Ortloff, R., and Joos, A., and Passegger, T*., Lane Keeping Based on Location Technology*, IEEE Transaction on Intelligent Transportation Systems, Vol. 6. No.3, September 2005, pages 351-356

51. Heimes, F., and Nagel, H. H., *Towards Active Machine-Vision-Based Driver Assistance for Urban Areas*, International Journal of Computer Vision 50(1) 2002, pages 5-34.

52. Goldbeck, J., Huertgen, B., Ernst, S., and Kelch, L*., Lane Following Combining Vision and DGPS,* Image and Vision Computing 18, 2000 pages 425-433.

53. Controls Tutorials for MATLAB & SIMULINK, Introduction: PID Controller Design, Available: <http://ctms.engin.umich.edu/CTMS/index.php?example=Introduction&section=ControlPID> 09/19/2019

54. MathWorks, Understanding Model Predictive Control, Available: <https://www.mathworks.com/videos/understanding-model-predictive-control-part-1-why-use-mpc--1526484715269.html> 09/19/2019

55. Standalone Power Converter, Report 2 , Available: <https://www.cefns.nau.edu/capstone/projects/EE/2018/OffgridConverter/report_2.html> 09/19/2019

56. Snider, J. M., *Automatic Steering Methods for Autonomous Automobile Path Tracking*, CMU-RI_TR_09-08, Robotics Institute Carnegie Mellon University, Pittsburgh, PA, February 2009.

57. MathWorks, Pure Pursuit Controller, Available: <https://www.mathworks.com/help/robotics/ug/pure-pursuit-controller.html> 09/19/2019

Appendix A Euler-Lagrange General Information

Find a function $y = f(x)$ *such that the functional* $F = \int_{x_1}^{x_2} F(x, y, y')dx$ *is stationary (is minimized or maximized). Along with boundary conditions of the form* $y(x_1) = y_1$ *and* $y(x_2) = y_2$.

Let $y(x)$ be a solution that makes F stationary and satisfies boundary conditions.

Introduce:

$$\beta(x) = \text{Arbitrary Function} \quad \& \quad \beta(x_1) = \beta(x_2) = 0 \tag{A.1}$$

Define:

$$\bar{y}(x) = y(x) + \epsilon\beta(x) \qquad \text{(A. 2)} \tag{A.2}$$

Where:
$\bar{y}$ = Variation of Variable y
y = A function that makes F stationary
β = Arbitrary function dependent on x
ϵ = Small variation coefficient

Proof that equation (A.1) satisfies the same Boundary Conditions as problem statement:

Applying Boundary Conditions (1) into equation (A.1) the problem simplifies to the original $y = f(x)$ problem.

$$\bar{y}(x_1) = y(x_1) + \epsilon\beta(x_1) \tag{A.3a}$$

$$\bar{y}(x_1) = y(x_1) \tag{A.3b}$$

$$\bar{y}(x_2) = y(x_2) + \epsilon\beta(x_2) \tag{A.3c}$$

$$\bar{y}(x_2) = y(x_2) \tag{A.3d}$$

Thus, solving for $\bar{y}(x)$ is sufficient to solve for $y(x)$. E.O.M.

Through introduction of equation (A.2), it is possible to change the problem from solving for $y(x)$ to solving for $\bar{y}(x)$. Thus, turning the problem in the following form:

Find a function (or family of functions) $\bar{y}$ *which makes the new functional* $F(\epsilon) = \int_{x_1}^{x_2} F(x, \bar{y}, \bar{y}')\ dx$ *stationary.*

Given that equation (A.2) makes $\bar{y}$ dependent on x, the integral of $F(\epsilon) = \int_{x_1}^{x_2} F(x, \bar{y}, \bar{y}')\ dx$ will provide a functional $F(\epsilon)$ that only depends on ϵ. For this reason, it is possible to make an optimization problem by setting:

$$\frac{dF}{d\epsilon} = 0 \tag{A.4a}$$

In optimization problems, it is necessary to evaluate the function (or functional) at an extrema point. For this situation, ϵ can be evaluated at zero, which will provide an extrema as follows:

$$\bar{y}(x) = y(x) + \epsilon\beta(x) \ \rightarrow \quad \bar{y}(x) = y(x) \tag{A.4b}$$

Provided the assumption of $y(x)$ is a solution that makes F is stationary. By setting ϵ to zero, the functional F has been optimized.

$$\left.\frac{dF}{d\epsilon}\right|_{\epsilon=0} = 0 \tag{A.4c}$$

To evaluate this expression, the definition of F is used which gives an integral equation to solve:

$$\left.\frac{d}{d\epsilon}\right|_{\epsilon=0} \int_{x_1}^{x_2} F(x, \bar{y}, \bar{y}')\, dx = 0 \tag{A.4d}$$

$$\int_{x_1}^{x_2} \left.\frac{d}{d\epsilon} F(x, \bar{y}, \bar{y}')\, dx\right|_{\epsilon=0} dx = 0 \tag{A.4e}$$

By replacing $F(x, \bar{y}, \bar{y}') = F$ & using the Chain Rule:

$$\int_{x_1}^{x_2} \left[\frac{\partial F}{\partial \bar{y}}\frac{\partial \bar{y}}{\partial \epsilon} + \frac{\partial F}{\partial \bar{y}'}\frac{\partial \bar{y}'}{\partial \epsilon}\right]_{\epsilon=0} dx = 0 \tag{A.4f}$$

Remark of equation (A.2) and its derivatives:

$$\bar{y}(x) = y(x) + \epsilon\beta(x) \tag{A.5a}$$

$$\bar{y}'(x) = y'(x) + \epsilon\beta'(x) \tag{A.5b}$$

$$\frac{\partial \bar{y}}{\partial \epsilon} = \beta(x) = \beta \tag{A.5c}$$

$$\frac{\partial \bar{y}'}{\partial \epsilon} = \beta'(x) = \beta' \tag{A.5d}$$

Plugging those into equation (A.4f):

$$\int_{x_1}^{x_2} \left[\frac{\partial F}{\partial \bar{y}}\beta + \frac{\partial F}{\partial \bar{y}'}\beta'\right]_{\epsilon=0} dx = 0 \tag{A.6a}$$

Splitting the integral into its two constituents, the second term $\frac{\partial F}{\partial \bar{y}'}\beta'$ can be simplified using integration by parts:

$$\int_{x_1}^{x_2} \frac{\partial F}{\partial \bar{y}'}\beta'\, dx = \frac{\partial F}{\partial \bar{y}'}\int \beta'\, dx - \int_{x_1}^{x_2} \int \beta' dx \frac{d}{dx}\left[\frac{\partial F}{\partial \bar{y}'}\right]\, dx \tag{A.6b}$$

By definition: $\int \beta' dx = \beta$

$$\int_{x_1}^{x_2} \frac{\partial F}{\partial \bar{y}'}\beta'\, dx = \frac{\partial F}{\partial \bar{y}'}[\beta]_{x_2}^{x_1} - \int_{x_1}^{x_2} \beta \frac{d}{dx}\left[\frac{\partial F}{\partial \bar{y}'}\right]\, dx \tag{A.6c}$$

Applying boundary conditions (1) for limit on the left term $\beta(x_1) = \beta(x_2) = 0$

$$\int_{x_1}^{x_2} \frac{\partial F}{\partial \bar{y}'}\beta'\, dx = -\int_{x_1}^{x_2} \beta \frac{d}{dx}\left[\frac{\partial F}{\partial \bar{y}'}\right]\, dx \tag{A.7}$$

Plugging Equation (A.7) back into Equation (A.6a)

$$\int_{x_1}^{x_2} \left[\frac{\partial F}{\partial \bar{y}}\beta - \beta \frac{d}{dx}\left[\frac{\partial F}{\partial \bar{y}'}\right]\right]_{\epsilon=0} dx = 0 \tag{A.8}$$

From Equation (A.2), it was stated that setting $\epsilon = 0$ yields $\bar{y} = y$, which was defined as an optimal solution for the functional. Thus, setting $\epsilon = 0$ into equation (A.8):

$$\int_{x_1}^{x_2} \frac{\partial F}{\partial y}\beta - \beta \frac{d}{dx}\left[\frac{\partial F}{\partial y'}\right] dx = 0 \tag{A.9}$$

Grouping similar terms, and expressing β as an arbitrary function of x:

$$\int_{x_1}^{x_2} \left[\frac{\partial F}{\partial y} - \frac{d}{dx}\frac{\partial F}{\partial y'}\right] \beta(x)\, dx = 0 \tag{A.10a}$$

This final equation is a product in between an arbitrary function $\beta(x)$ and a functional. Therefore, for the equation (A.10a) to be true for any arbitrary $\beta(x)$. The following has to be true:

$$\left[\frac{\partial F}{\partial y} - \frac{d}{dx}\frac{\partial F}{\partial y'}\right] = 0 \tag{A.10b}$$

Therefore: If $y(x)$ makes F stationary, then $y(x)$ must satisfy the previous equation know as Euler-Lagrange Equation.